PHYSICAL REVIEW D **89,** 094018 (2014)

Dalitz plot studies of $D^0 \to K^0_S\pi^+\pi^-$ decays in a factorization approach

J.-P. Dedonder,[1] R. Kamiński,[2] L. Leśniak,[2,*] and B. Loiseau[1]

[1]*Sorbonne Universités, Université Pierre et Marie Curie, Sorbonne Paris Cité, Université Paris Diderot, et IN2P3-CNRS, UMR 7585, Laboratoire de Physique Nucléaire et de Hautes Énergies, 4 place Jussieu, 75252 Paris, France*

[2]*Division of Theoretical Physics, The Henryk Niewodniczański Institute of Nuclear Physics, Polish Academy of Sciences, 31-342 Kraków, Poland*

(Received 12 March 2014; published 21 May 2014)

The presently available high-statistics data of the $D^0 \to K^0_S\pi^+\pi^-$ processes measured by the Belle and *BABAR* collaborations are analyzed within a quasi-two-body factorization framework. Starting from the weak effective Hamiltonian, tree and annihilation amplitudes build up the $D^0 \to K^0_S\pi^+\pi^-$ decay amplitude. Two of the three final-state mesons are assumed to form a single scalar, vector or tensor state originating from a quark-antiquark pair so that the factorization hypothesis can be applied. The meson-meson final state interactions are described by $K\pi$ and $\pi\pi$ scalar and vector form factors for the S and P waves and by relativistic Breit-Wigner formulas for the D waves. A combined χ^2 fit to a Belle Dalitz plot density distribution, to the total experimental branching fraction and to the $\tau^- \to K^0_S\pi^-\nu_\tau$ decay data, is carried out to fix the 33 free parameters. These are mainly related to the strengths of the scalar form factors and to unknown meson to meson transition form factors at a large momentum transfer squared equal to the D^0 mass squared. A good overall agreement to the Belle Dalitz plot density distribution is achieved. Another set of parameters fits equally well the *BABAR* collaboration Dalitz plot model. The parameters of both fits are close, following from similar Dalitz density distribution data for both collaborations. The corresponding one-dimensional effective mass distributions display the contributions of the ten quasi-two-body channels entering our $D^0 \to K^0_S\pi^+\pi^-$ decay amplitude. The branching fractions of the dominant channels compare well with those of the isobar Belle or *BABAR* models. The lower-limit values of the branching fractions of the annihilation amplitudes are significant. Built upon experimental data from other processes, the unitary $K\pi$ and $\pi\pi$ scalar form factors, entering our decay amplitude and satisfying analyticity and chiral symmetry constraints, are furthermore constrained by the present Dalitz plot analysis. Our $D^0 \to K^0_S\pi^+\pi^-$ decay amplitude could be a useful input for determinations of D^0-$\bar{D}^0$ mixing parameters and of the Cabibbo-Kobayashi-Maskawa angle γ (or ϕ_3).

DOI: 10.1103/PhysRevD.89.094018 PACS numbers: 13.25.Hw, 13.75.Lb

I. INTRODUCTION

Measurements of the D^0-$\bar{D}^0$ mixing parameters, through Dalitz-plot time dependent amplitude analyses of the weak process $D^0 \to K^0_S\pi^+\pi^-$, have been performed by the Belle [1] and *BABAR* [2] collaborations. These studies could help in the understanding of the origin of mixing and may indicate the possible presence of new physics contribution. No CP violation in these D^0 decays [3,4] has yet been found, in agreement with the very small value predicted by the standard model in the charm sector. The Cabibbo-Kobayashi-Maskawa (CKM) angle γ (or ϕ_3) has been evaluated from the analyses of the $B^\pm \to D^0K^\pm$, $D^0 \to K^0_S\pi^+\pi^-$ decays [5–10]. A good knowledge of the final state meson interactions is important to reduce the uncertainties in the determination of the D^0-$\bar{D}^0$ mixing parameters and of the angle γ. The very rich structures seen in the Dalitz plot spectra point to the complexity of these final state strong interactions.

The experimental analyses [1,2] rely mainly on the use of the isobar model. In this approach, one can take into account the many existing resonances coupled to the interacting pairs of mesons. However, the corresponding decay amplitudes are not unitary and unitarity is not preserved in the three-body decay channels; it is also violated in the two-body subchannels. Furthermore, it is difficult to differentiate the S-wave amplitudes from the nonresonant background terms. Their interferences are noteworthy and then some two-body branching fractions, extracted from the data, could be unreliable. The isobar model is tractable but it has many free parameters: at least two fitted parameters for each amplitude and for example, the Belle collaboration in Ref. [1] has used 40 fitted parameters and the *BABAR* collaboration 43 in Ref. [2].

Imposing unitarity for three-body strong interactions in a wide range of meson-meson effective masses is difficult. Some three-body unitarity corrections have been evaluated in Ref. [11] for $D^0 \to \pi^0\pi^+\pi^-$ decays and in Ref. [12] for $D^+ \to K^-\pi^+\pi^+$. In a unitary coupled-channel model Ref. [11] has shown that two-body rescattering terms could

*leonard.lesniak@ifj.edu.pl

be important. They find that the decay amplitudes of the unitary model can be rather different from those of the isobar model. In Ref. [12] the three-body unitarity is formulated with an integral equation inspired by the Faddeev formalism. There, they sum up a perturbation series and find that three-body effects important close to threshold fade away at higher energies. In the present work, as a first step, we require two-body unitarity in the D-decay amplitudes with the $K^0_S\pi^\pm$ final state in S wave and with the $\pi^+\pi^-$ final state in S and P waves. According to the experimental works [1,2], the sum of the branching fractions corresponding to these amplitudes yields an important part of the total branching fraction of the $D^0 \to K^0_S\pi^+\pi^-$ decay.

The two-body QCD factorization has been applied with success to charmless nonleptonic B decays (see e.g. Ref. [13]). For the D meson the charm quark mass m_c is lighter than the bottom quark mass by about a factor of 3. The c quark mass is too high to apply chiral perturbation theory and too light to use heavy quark expansion approaches. One expects nonperturbative D-decay contributions of order $\Lambda_{\rm QCD}/m_c$ to be more important than in B decays. Consequently, the factorization hypothesis could be less reliable. Nevertheless, following the initial articles of Bauer, Stech, and Wirbel [14,15] the assumption of factorization has been applied successfully to D decays in several recent papers [16–19]. The Wilson coefficients are treated as phenomenological parameters to account for possible important nonfactorizable corrections [20]. An alternative diagrammatic approach for the description of hadronic charmed meson decays into two-body has been the support of the works presented in Refs. [21] and [22].

In the framework of the quasi-two-body factorization approximation [13] and of the extension of a program devoted to the understanding of rare three-body B decays [23–27], we analyze the presently available $D^0 \to K^0_S\pi^+\pi^-$ data. So far no factorization scheme has been worked out for three-body decays. Then, as in our previous studies, we assume that two of the three final-state mesons forms a single state which originates from a quark-antiquark, $q\bar{q}$, pair. Such a hypothesis leads to quasi-two-body final states to which the factorization procedure is applied. The three-meson final states $K^0_S\pi^+\pi^-$ are here supposed to be formed by the following quasi-two-body pairs, $[K^0_S\pi^+]_L\pi^-$, $[K^0_S\pi^-]_L\pi^+$ and $K^0_S[\pi^+\pi^-]_L$, where two of the three mesons form a state in $L = S$, P or D wave. The $D^0 \to K^0_S\pi^+\pi^-$ decay amplitudes, derived from the weak effective Hamiltonian, have contributions from tree diagrams but none from penguin or W-loop diagrams. There are also annihilation amplitudes arising from W-meson exchange between the D^0 quark constituents. The amplitudes corresponding to the $c \to su\bar{d}$ transition are Cabibbo favored (CF) while those with $c \to du\bar{s}$ are doubly Cabibbo suppressed (DCS).

In the factorization approach, the CF and DCS amplitudes are expressed as superpositions of appropriate effective coefficients and two products of two transition matrix elements. For the CF tree amplitudes, the first and second product correspond to the transition matrix element between the D^0 and $[\bar{K}^0\pi^-]_L$ or $[\pi^+\pi^-]_L$ state multiplied by the transition matrix element between the vacuum and the π^+ (proportional to the pion decay constant) or the $\bar{K}^0$ (proportional to the kaon decay constant), respectively. For the DCS tree amplitude these products correspond to the transition between the D^0 and π^- or $[\pi^-\pi^+]_L$ state multiplied by the transition between the vacuum and the $[K^0\pi^+]_L$ (proportional to the kaon-pion form factor) or the K^0 (proportional to the kaon decay constant), respectively. In the latter case, in the $K^0\pi$ center-of-mass frame, the bilinear quark current involved forces the $[K^0\pi^+]$ pair to be in a $L = S$ or P wave. For the CF (DCS) annihilation amplitudes the products correspond to the transition between the π or $\bar{K}^0(K^0)$ and $[\bar{K}^0\pi^-]_L([K^0\pi^+]_L)$ or $[\pi^+\pi^-]_L$ state, multiplied by the transition between the vacuum and the D^0 (proportional to the D^0 decay constant), respectively.

We presume that the transition of the D^0 to the meson pairs $[\bar{K}^0\pi^-]_L$ or $[\pi^+\pi^-]_L$ goes first through the dominant intermediate resonance R_L of these pairs. For the $[\bar{K}^0\pi^-]_L$ pair, we take, $R_S[\bar{K}^0\pi^-] = K^*_0(1430)^-$, $R_P[\bar{K}^0\pi^-] = K^*(892)^-$, $R_D[\bar{K}^0\pi^-] = K^*_2(1430)^-$ and for the $[\pi^+\pi^-]_L$ pair, $R_S[\pi^+\pi^-] = f_0(980)$, $R_P[\pi^+\pi^-] = \rho(770)^0$ and $R_D[\pi^+\pi^-] = f_2(1270)$. We further calculate the $D^0 \to \bar{K}^0\pi^-$ or $\pi^+\pi^-$ matrix elements as products of the $D^0 \to R_L[\bar{K}^0\pi^-]$ or $R_L[\pi^+\pi^-]$ transition form factors by the relevant vertex function describing the decay of the $[\bar{K}^0\pi]_L$ or $[\pi\pi]_L$ states into the final meson pair. The vertex functions are in turn expected to be proportional to the kaon-pion or pion scalar form factor for the S wave, to the vector form factor for the P wave and to a relativistic Breit-Wigner formula for the D wave. For the CF (DCS) annihilation amplitudes we follow the same steps as for the tree amplitudes but for the replacement of D^0 by π or $\bar{K}^0(K^0)$.

The meson-meson final state interactions for the S and P waves are then described in terms of experimentally and theoretically constrained $K\pi$ and $\pi\pi$ scalar and vector form factors. Using unitarity, analyticity and chiral symmetry constraints, the scalar form factors have been been derived in Ref. [25] for the $K\pi$ case and in Ref. [27] for the pion one. They are single unitary functions describing the two scalar resonances $K^*_0(800)$ (or κ), $K^*_0(1430)$ and the three scalar resonances, $f_0(500)$, $f_0(980)$ and $f_0(1400)$ present in the $K^0_S\pi^\pm$ and $\pi^+\pi^-$ interactions, respectively. The vector form factors are based on the Belle analyses of the $\tau^- \to K^0_S\pi^-\nu_\tau$ [28] and of the $\tau^- \to \pi^-\pi^0\nu_\tau$ [29] decay processes. We also include the amplitude describing the $D^0 \to \omega(782)K^0_S$ channel followed by the $\omega(782) \to \pi^+\pi^-$ decay. Relativistic Breit-Wigner formulas are introduced to describe the final state D wave meson-meson interactions. The undetermined parameters of our $D^0 \to K^0_S\pi^+\pi^-$ decay amplitudes, mainly related to the strength of the $[K\pi]_S$ and

$[\pi\pi]_S$ scalar form factors and to the unknown meson to meson transition form factors, are obtained through a χ^2 fit to the Dalitz plot data sample of the 2010 Belle collaboration analysis [10,30]. We also fit the Dalitz plot density of the *BABAR* collaboration model [31].

The paper is structured as follows. Section II describes formally the amplitudes calculated in the framework of the quasi-two-body factorization approach. Section III provides a practical formulation of these amplitudes by introducing combinations of some of them more amenable to numerical calculations. A discussion of the branching fractions is also given there. Section IV lists the necessary input for the evaluation of the amplitudes. Results are presented and discussed in Sec. V while Sec. VI summarizes the outcome of this analysis and Sec. VII proposes some conclusions and perspectives.

II. THE $D^0 \to K^0_S\pi^+\pi^-$ DECAY AMPLITUDES IN FACTORIZATION FRAMEWORK

The decay amplitudes for the $D^0 \to K^0_S\pi^+\pi^-$ process can be evaluated as matrix elements of the effective weak Hamiltonian [32]

$$H_{\rm eff} = \frac{G_F}{\sqrt{2}} V_{\rm CKM}[C_1(\mu)O_1(\mu) + C_2(\mu)O_2(\mu)] + \text{H.c.}, \quad (1)$$

where the coefficients $V_{\rm CKM}$ are given in terms of Cabibbo-Kobayashi-Maskawa quark-mixing matrix elements and G_F denotes the Fermi coupling constant. The $C_i(\mu)$ are the Wilson coefficients of the four-quark operators $O_i(\mu)$ at a renormalization scale μ, chosen to be equal to the c-quark mass m_c. The left-handed current-current operators $O_{1,2}(\mu)$ arise from W-boson exchange.

The transition matrix elements that occur in the present work require two specific values of the $V_{\rm CKM}$ coupling matrix elements:

$$\Lambda_1 \equiv V^*_{cs}V_{ud} \quad \text{and} \quad \Lambda_2 \equiv V^*_{cd}V_{us}. \quad (2)$$

The amplitudes are functions of the Mandelstam invariants

$$s_\pm = m^2_\pm = (p_0 + p_\pm)^2, \quad s_0 = m^2_0 = (p_+ + p_-)^2, \quad (3)$$

where p_0, p_+ and p_- are the four momenta of the K^0_S, π^+ and π^- mesons, respectively. Energy-momentum conservation implies

$$p_{D^0} = p_0 + p_+ + p_- \quad \text{and}$$
$$s_0 + s_+ + s_- = m^2_{D^0} + m^2_{K^0} + 2m^2_\pi, \quad (4)$$

where p_{D^0} is the D^0 four momentum and m_{D^0}, m_{K^0} and m_π denote the D^0, K^0 and charged pion masses.

The full amplitude is the superposition of two tree Cabibbo favored and doubly Cabibbo suppressed amplitudes, $\mathcal{T}^{\rm CF}(s_0, s_-, s_+)$ and $\mathcal{T}^{\rm DCS}(s_0, s_-, s_+)$ and of two annihilation (i.e., exchange of W meson between the c and $\bar{u}$ quarks of the D^0) CF and DCS amplitudes, $\mathcal{A}^{\rm CF}(s_0, s_-, s_+)$ and $\mathcal{A}^{\rm DCS}(s_0, s_-, s_+)$. Thus, one writes the full amplitude as

$$\begin{aligned}\mathcal{M}(s_0, s_-, s_+) &= \langle K^0_S(p_0)\pi^+(p_+)\pi^-(p_-)|H_{\rm eff}|D^0(p_{D^0})\rangle \\ &= \mathcal{T}^{\rm CF}(s_0, s_-, s_+) + \mathcal{T}^{\rm DCS}(s_0, s_-, s_+) \\ &\quad + \mathcal{A}^{\rm CF}(s_0, s_-, s_+) + \mathcal{A}^{\rm DCS}(s_0, s_-, s_+), \quad (5)\end{aligned}$$

where the CF amplitudes are proportional to Λ_1 and the DCS ones to Λ_2. Although the three variables s_0, s_-, s_+ appear as arguments of the amplitudes, because of the relation (4) all amplitudes depend only on two of them.

Assuming that the factorization approach [13,20,32,33] with quasi-two-body $[K\pi]_L\pi$ or $K[\pi\pi]_L$, $L = S, P, D$, states holds, the tree CF amplitudes, $T^{\rm CF}$, read, with $|0\rangle$ indicating the vacuum state,

$$\begin{aligned}T^{\rm CF}(s_0, s_-, s_+) &= \frac{G_F}{2}\Lambda_1 \sum_{L=S,P,D} [a_1(m_c)\langle[\bar{K}^0(p_0)\pi^-(p_-)]_L|(\bar{s}c)_{V-A}|D^0(p_{D^0})\rangle \cdot \langle\pi^+(p_+)|(\bar{u}d)_{V-A}|0\rangle \\ &\quad + a_2(m_c)\langle\bar{K}^0(p_0)|(\bar{s}d)_{V-A}|0\rangle \cdot \langle[\pi^+(p_+)\pi^-(p_-)]_L|(\bar{u}c)_{V-A}|D^0(p_{D^0})\rangle] \\ &= \sum_{L=S,P,D} T^{\rm CF}_{[\bar{K}^0\pi^-]_L\pi^+}(s_0, s_-, s_+) + \sum_{L=S,P,D} T^{\rm CF}_{\bar{K}^0[\pi^+\pi^-]_L}(s_0, s_-, s_+) \\ &= T^{\rm CF}_{[\bar{K}^0\pi^-]\pi^+}(s_0, s_-, s_+) + T^{\rm CF}_{\bar{K}^0[\pi^+\pi^-]}(s_0, s_-, s_+). \quad (6)\end{aligned}$$

In deriving Eq. (6) small CP violation effects in K^0_S decays are neglected and we use

$$|K^0_S\rangle \approx \frac{1}{\sqrt{2}}(|K^0\rangle + |\bar{K}^0\rangle). \quad (7)$$

At leading order in the strong coupling constant α_S, the effective QCD factorization coefficients $a_1(m_c)$ and $a_2(m_c)$ are expressed as

$$a_1(m_c) = C_1(m_c) + \frac{C_2(m_c)}{N_C}, \qquad a_2(m_c) = C_2(m_c) + \frac{C_1(m_c)}{N_C}, \quad (8)$$

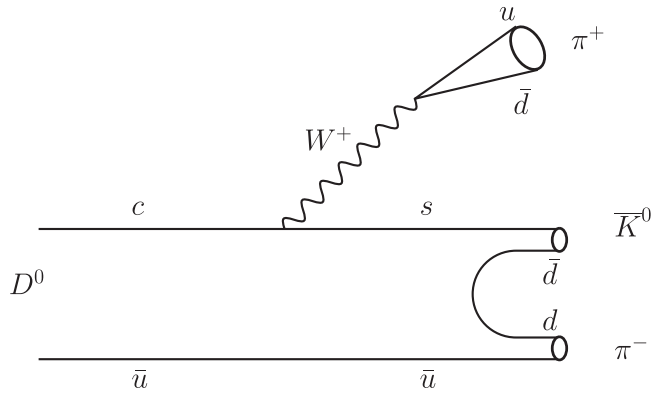

FIG. 1. Tree diagram for Cabibbo favored amplitudes with $[\bar{K}^0\pi^-]\pi^+$ final states.

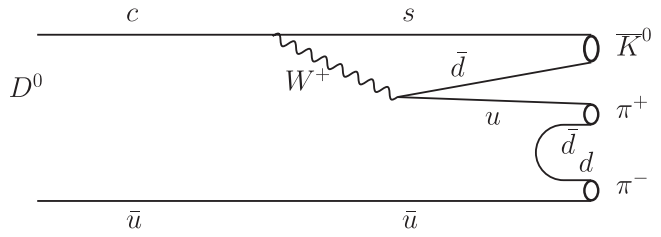

FIG. 2. As in Fig. 1 but for $\bar{K}^0[\pi^+\pi^-]$ final states.

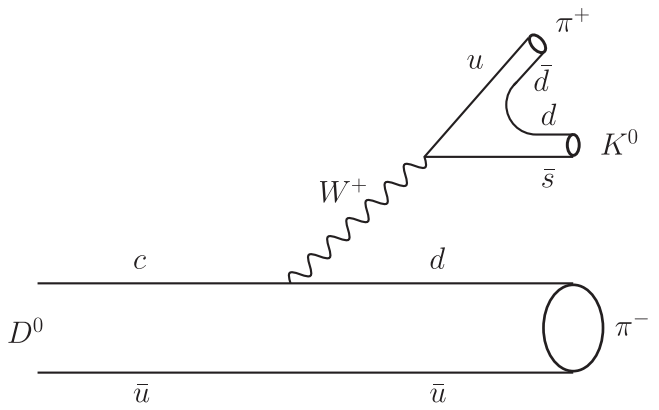

FIG. 3. Tree diagram for the doubly Cabibbo suppressed amplitude with $[K^0\pi^+]\pi^-$ final states.

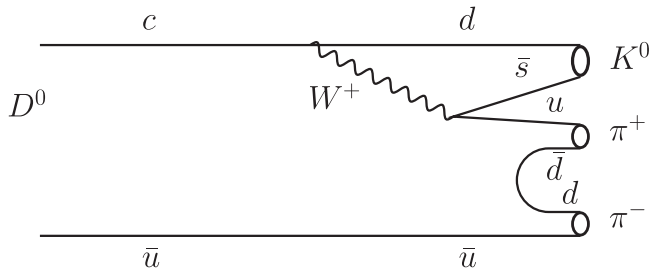

FIG. 4. As in Fig. 3 but for $K^0[\pi^+\pi^-]$ final states.

where $N_C = 3$ is the number of colors. Higher order vertex and hard scattering corrections are not discussed in the present work and we introduce effective values for these coefficients (see Sec. IV). From now on, the simplified notation $a_1 \equiv a_1(m_c)$ and $a_2 \equiv a_2(m_c)$ will be used. In Eq. (6), we have introduced the short-hand notation

$$(\bar{q}q)_{V-A} = \bar{q}\gamma(1-\gamma_5)q \tag{9}$$

which will be used throughout the text. The amplitudes $T^{\rm CF}_{[\bar{K}^0\pi^-]\pi^+}(s_0, s_-, s_+)$ and $T^{\rm CF}_{\bar{K}^0[\pi^+\pi^-]}(s_0, s_-, s_+)$ are illustrated diagrammatically in Figs. 1 and 2.

Similarly, the DCS tree amplitudes, $T^{\rm DCS}$, illustrated by the diagrams shown in Figs. 3 and 4, read

$$\begin{aligned} T^{\rm DCS}(s_0, s_-, s_+) &= \frac{G_F}{2}\Lambda_2 \sum_{L=S,P,D} [a_1\langle[K^0(p_0)\pi^+(p_+)]_L|(\bar{u}s)_{V-A}|0\rangle \cdot \langle\pi^-(p_-)|(\bar{d}c)_{V-A}|D^0(p_{D^0})\rangle + a_2\langle K^0(p_0)|(\bar{d}s)_{V-A}|0\rangle \\ &\quad \cdot \langle[\pi^+(p_+)\pi^-(p_-)]_L|(\bar{u}c)_{V-A}|D^0(p_{D^0})\rangle] \\ &= \sum_{L=S,P,D} T^{\rm DCS}_{[K^0\pi^+]_L\pi^-}(s_0, s_-, s_+) + \sum_{L=S,P,D} T^{\rm DCS}_{K^0[\pi^-\pi^+]_L}(s_0, s_-, s_+) \\ &= T^{\rm DCS}_{[K^0\pi^+]\pi^-}(s_0, s_-, s_+) + T^{\rm DCS}_{K^0[\pi^-\pi^+]}(s_0, s_-, s_+). \end{aligned} \tag{10}$$

A similar derivation for the CF annihilation amplitudes, $A^{\rm CF}$, illustrated by the diagram in Fig. 5, yields

$$\begin{aligned} A^{\rm CF}(s_0, s_-, s_+) &= \frac{G_F}{2}\Lambda_1 a_2 \sum_{L=S,P,D} [\langle[\bar{K}^0(p_0)\pi^-(p_-)]_L\pi^+(p_+)|(\bar{s}d)_{V-A}|0\rangle \\ &\quad + \langle\bar{K}^0(p_0)[\pi^-(p_-)\pi^+(p_+)]_L|(\bar{s}d)_{V-A}|0\rangle] \cdot \langle 0|(\bar{c}u)_{V-A}|D^0(p_{D^0})\rangle \\ &= \sum_{L=S,P,D} A^{\rm CF}_{[\bar{K}^0\pi^-]_L\pi^+}(s_0, s_-, s_+) + \sum_{L=S,P,D} A^{\rm CF}_{\bar{K}^0[\pi^+\pi^-]_L}(s_0, s_-, s_+) \\ &= A^{\rm CF}_{[\bar{K}^0\pi^-]\pi^+}(s_0, s_-, s_+) + A^{\rm CF}_{\bar{K}^0[\pi^+\pi^-]}(s_0, s_-, s_+). \end{aligned} \tag{11}$$

The corresponding DCS annihilation amplitudes, $A^{\rm DCS}$, (see Fig. 6), obtained from Eq. (11) with the substitutions $\Lambda_1 \Rightarrow \Lambda_2$, $\pi^+ \Leftrightarrow \pi^-$, $\bar{K}^0 \Rightarrow K^0$ and $d \Leftrightarrow s$, read

$$\begin{aligned} A^{\rm DCS}(s_0,s_-,s_+) &= \frac{G_F}{2}\Lambda_2 a_2 \sum_{L=S,P,D} [\langle [K^0(p_0)\pi^+(p_+)]_L \pi^-(p_-)|(\bar{d}s)_{V-A}|0\rangle \\ &\quad + \langle K^0(p_0)[\pi^+(p_+)\pi^-(p_-)]_L|(\bar{d}s)_{V-A}|0\rangle] \cdot \langle 0|(\bar{c}u)_{V-A}|D^0(p_{D^0})\rangle \\ &= \sum_{L=S,P,D} A^{\rm DCS}_{[K^0\pi^+]_L\pi^-}(s_0,s_-,s_+) + \sum_{L=S,P,D} A^{\rm DCS}_{K^0[\pi^-\pi^+]_L}(s_0,s_-,s_+) \\ &= A^{\rm DCS}_{[K^0\pi^+]\pi^-}(s_0,s_-,s_+) + A^{\rm DCS}_{K^0[\pi^-\pi^+]}(s_0,s_-,s_+). \end{aligned} \tag{12}$$

Let us now review in detail the 28 amplitudes that build up the total $D^0 \to K^0_S\pi^+\pi^-$ amplitude defined in Eq. (5). Indeed, for each amplitude in Eq. (5) there are three ($L = S$, P, D) contributions for the $[K\pi]\pi$ states and three for the $K[\pi\pi]$ ones as can be seen from Eqs. (6), (10)–(12). To these 24 amplitudes one has to add the four contributions in which the $[\pi\pi]_P$ pair in the $K[\pi\pi]$ final state originates from the $\omega(782) \to \pi^+\pi^-$ decay.

A. Cabibbo favored amplitudes

1. The $[K^0_S\pi^-]_S\pi^+$ and $K^0_S[\pi^+\pi^-]_S$ amplitudes

Starting from Eq. (6) we build now the expression of the different CF amplitudes following a derivation similar to that described in detail in Ref. [27] (see, in particular, Appendix A of Ref. [27] and Sec. II C of this paper where an analogous explicit derivation for the annihilation amplitudes is presented). The $[K^0_S\pi^-]_S\pi^+$ amplitude is

$$\begin{aligned} T^{\rm CF}_{[\bar{K}^0\pi^-]_S\pi^+}(s_0,s_-,s_+) &= -\frac{G_F}{2} a_1 \Lambda_1 \chi_1 (m^2_{D^0} - s_-) \\ &\quad \times f_\pi F_0^{D^0 R_S[\bar{K}^0\pi^-]}(m^2_\pi) F_0^{\bar{K}^0\pi^-}(s_-) \\ &\equiv T_1. \end{aligned} \tag{13}$$

The transition form factor $F_0^{D^0 R_S[\bar{K}^0\pi^-]}(m^2_\pi)$ is dominated by the $K^*_0(1430)^-$ resonance. It is real in the kinematical range considered here. The form factor $F_0^{\bar{K}^0\pi^-}(s_-)$ includes the contribution of the $K^*_0(800)^-$ (or κ^-) and $K^*_0(1430)^-$ resonances.

The $K^0_S[\pi^+\pi^-]_S$ amplitude reads

$$\begin{aligned} T^{\rm CF}_{\bar{K}^0[\pi^+\pi^-]_S}(s_0,s_-,s_+) &= -\frac{G_F}{2} a_2 \Lambda_1 \chi_2 (m^2_{D^0} - s_0) \\ &\quad \times f_{K^0} F_0^{D^0 R_S[\pi^+\pi^-]}(m^2_{K^0}) F_0^{\pi^+\pi^-}(s_0) \\ &\equiv T_2, \end{aligned} \tag{14}$$

where the transition form factor $F_0^{D^0 R_S[\pi^+\pi^-]}(m^2_{K^0})$ is assumed to be dominated by the $f_0(980)$ resonance. It is also purely real.

In the equations above, f_π and f_{K^0} represent the pion and K^0 decay constants. The $[\pi\pi]$ S-wave form factor $F_0^{\pi^+\pi^-}(s_0)$ includes the contribution of the $f_0(500)$ (or σ), $f_0(980)$ and $f_0(1400)$ resonances. The $K\pi$ and $\pi\pi$ scalar form factors $F_0^{\bar{K}^0\pi^-}(s_-)$ and $F_0^{\pi^+\pi^-}(s_0) = \sqrt{\frac{2}{3}}\,\Gamma_1^{n*}(s_0)$ will be built following the methods discussed in Refs. [25] and [27].

In Eqs. (13) and (14) the factors χ_1 and χ_2 are related to the strength of the $[K\pi]_S$ and $[\pi\pi]_S$ scalar form factors, respectively. As just mentioned these form factors receive contributions from different resonances. If a resonance $R_S[K\pi]$ or $R_S[\pi\pi]$ was dominant χ_1 and χ_2 could be evaluated in terms of the decay constant of these resonances. As shown in Eq. (A.8) of Ref. [27] and as discussed in Sec. V of the present paper, their values could be estimated from the dominating resonance decay properties. Here, there is no dominant resonance then χ_1 and χ_2 are taken as complex constants to be fitted.

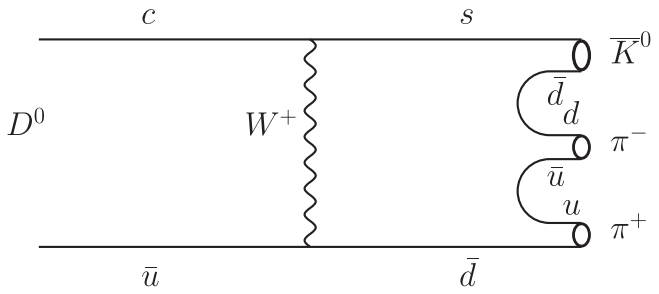

FIG. 5. Diagram for the Cabibbo favored annihilation (W-exchange) amplitudes.

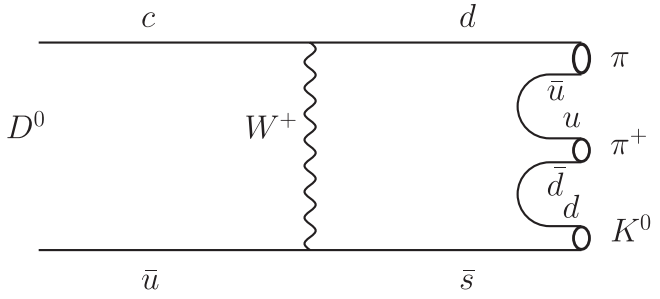

FIG. 6. As in Fig. 5 but for the doubly Cabibbo suppressed annihilation (W-exchange) amplitudes.

2. The $[K_S^0\pi^-]_P\pi^+$ and $K_S^0[\pi^+\pi^-]_P$ amplitudes

The $[K_S^0\pi^-]_P\pi^+$ amplitude reads, with $K^{*-} \equiv K^*(892)^-$,

$$T^{\rm CF}_{[\bar{K}^0\pi^-]_P\pi^+}(s_0,s_-,s_+) = \frac{G_F}{2}a_1\Lambda_1\frac{f_\pi}{f_{K^{*-}}}\left(s_0 - s_+ + (m_{K^0}^2 - m_\pi^2)\frac{m_{D^0}^2 - m_\pi^2}{s_-}\right)A_0^{D^0R_P[\bar{K}^0\pi^-]}(m_\pi^2)F_1^{\bar{K}^0\pi^-}(s_-) \equiv T_3, \quad (15)$$

where $A_0^{D^0R_P[\bar{K}^0\pi^-]}(m_\pi^2)$ denotes the form factor describing the D^0 to $[\bar{K}^0\pi^-]_P$ transition, largely dominated by the $K^*(892)^-$ resonance. The form factor $F_1^{\bar{K}^0\pi^-}(s_-)$ includes *a priori* the contribution of the $K^*(892)^-$, $K_1(1410)^-$ and $K^*(1680)^-$ resonances [28] (see Sec. IV). It has been discussed notably in Refs. [25], [34], and [35].

The $K_S^0[\pi^+\pi^-]_P$ amplitude is given by

$$\begin{aligned} &T^{\rm CF}_{\bar{K}^0[\pi^+\pi^-]_P}(s_0,s_-,s_+) \\ &= \frac{G_F}{2}a_2\Lambda_1\frac{f_{K^0}}{f_\rho}(s_- - s_+)A_0^{D^0R_P[\pi^+\pi^-]}(m_{K^0}^2)F_1^{\pi^+\pi^-}(s_0) \\ &\equiv T_4, \end{aligned} \quad (16)$$

where the transition form factor $A_0^{D^0R_P[\pi^+\pi^-]}(m_{K^0}^2)$ is dominated by the $\rho(770)^0$ resonance. The form factor $F_1^{\pi^+\pi^-}(s_0)$ which includes *a priori* the contributions of the $\rho(770)^0$, $\rho(1450)^0$ and $\rho(1700)^0$ is the same as that introduced in Ref. [27], following the analysis in Ref. [29] based on a Gounaris-Sakurai form with parameters extracted from the third column of their Table VII. Alternatively we also use one of the unitary parametrizations derived by Hanhart in Ref. [36]. Since the K^{*-} and $\rho(770)^0$ are dominating resonances, we use in Eqs. (15) and (16), $f_{K^{*-}}$ and f_ρ to represent the $R_P[\bar{K}^0\pi^-]$ and $R_P[\pi^+\pi^-]$ decay constants (here, f_ρ denotes the charged ρ decay constant).

The $D^0 \to \bar{K}^0[\pi^+\pi^-]_P$ decay can also proceed through the two-step process $D^0 \to \bar{K}^0\omega$ followed by the decay $\omega \to \pi^+\pi^-$; it yields an amplitude similar to that of the $D^0 \to \bar{K}^0[\pi^+\pi^-]_P$ process with the replacement of the $[\pi^+\pi^-]_P$ pair by the ω and the subsequent decay $\omega \to \pi^+\pi^-$, which violates isospin conservation. Thus, this term has to be added to the P-wave amplitude. Defining

$$\begin{aligned} &\langle\bar{K}^0(p_0)[\pi^+(p_+)\pi^-(p_-)]_\omega|H_{\rm eff}|D^0(p_D)\rangle \\ &\quad = T^{\rm CF}_{\bar{K}^0[\pi^+\pi^-]_\omega}(s_0,s_-,s_+), \end{aligned} \quad (17)$$

one has, in the quasi-two-body factorization,

$$\begin{aligned} &T^{\rm CF}_{\bar{K}^0[\pi^+\pi^-]_\omega}(s_0,s_-,s_+) \\ &\quad = \frac{G_F}{\sqrt{2}}\Lambda_1 a_2\langle\bar{K}^0(p_0)|(\bar{s}d)_{V-A}|0\rangle \\ &\qquad \cdot\langle[\pi^+(p_+)\pi^-(p_-)]_\omega|(\bar{u}c)_{V-A}|D^0(p_{D^0})\rangle \end{aligned} \quad (18)$$

with

$$\langle\bar{K}^0(p_0)|(\bar{s}d)_{V-A}|0\rangle = if_{K^0}p_0, \quad (19)$$

and

$$\begin{aligned} &\langle[\pi^+(p_+)\pi^-(p_-)]_\omega|(\bar{u}c)_{V-A}|D^0(p_{D^0})\rangle \\ &\quad = \frac{1}{\sqrt{2}}G_{\omega\pi^+\pi^-}(s_0)\epsilon\cdot(p^+ - p^-) \\ &\qquad \times\langle\omega(p_+ + p_-)|(\bar{u}c)_{V-A}|D^0(p_{D^0})\rangle. \end{aligned} \quad (20)$$

where ϵ represents the four-vector polarization of the ω meson. The matrix element in the above equation reads [see, e.g., Eq. (24) of Ref. [33]]

$$\begin{aligned} \langle\omega(s_0)|(\bar{u}c)_{V-A}|D^0(p_{D^0})\rangle &= -i\frac{2m_\omega(\epsilon^*\cdot p_D)}{p_0^2}p_0A_0^{D^0\omega}(p_0^2) \\ &\quad + \text{“other terms”}, \end{aligned} \quad (21)$$

where the “other terms” do not contribute when they are multiplied by Eq. (19). The $\omega\pi^+\pi^-$ vertex function is given by

$$G_{\omega\pi^+\pi^-}(p_+ + p_-) = \frac{g_{\omega\pi\pi}}{m_\omega^2 - s_0 - im_\omega\Gamma_\omega}, \quad (22)$$

where the expression of the coupling coefficient $g_{\omega\pi\pi}$ is given in Sec. IV and Γ_ω is the ω total width. One eventually arrives at

$$\begin{aligned} &T^{\rm CF}_{\bar{K}^0[\pi^+\pi^-]_\omega}(s_0,s_-,s_+) \\ &= \frac{G_F}{2}a_2\Lambda_1\frac{f_{K^0}}{\sqrt{2}}m_\omega(s_- - s_+)\frac{g_{\omega\pi\pi}A_0^{D^0\omega}(m_{K^0}^2)}{m_\omega^2 - s_0 - im_\omega\Gamma_\omega} \equiv T_5. \end{aligned} \quad (23)$$

3. The $[K_S^0\pi^-]_D\pi^+$ and $K_S^0[\pi^+\pi^-]_D$ amplitudes

One has finally to evaluate the $[K_S^0\pi^-]_D\pi^+$ amplitude associated to the $K_2^{*-} \equiv K_2^{*-}(1430)$ resonance for the $[K_S^0\pi^-]_D$ states and the $K_S^0[\pi^+\pi^-]_D$ one related to the $f_2 \equiv f_2(1270)$ for the $[\pi^+\pi^-]_D$ states. With the notation $m_{K_2^*} \equiv m_{K_2^{*-}(1430)}$, the amplitude related to the K_2^{*-} resonance reads

$$\begin{aligned} T^{\rm CF}_{[\bar{K}^0\pi^-]_D\pi^+}(s_0,s_-,s_+) &= -\frac{G_F}{2}a_1\Lambda_1 f_\pi F^{D^0R_D[\bar{K}^0\pi^-]}(s_-,m_\pi^2) \\ &\quad \times\frac{g_{K_2^{*-}K_S^0\pi^-}D(\mathbf{p}_1,\mathbf{p}_+)}{m_{K_2^*}^2 - s_- - im_{K_2^*}\Gamma_{K_2^*}} \\ &\equiv T_6, \end{aligned} \quad (24)$$

where $g_{K_2^{*-}K_S^0\pi^-}$ is the K_2^{*-} coupling constant to the $K_S^0\pi^-$ pair since the width $\Gamma_{K_2^*}$ will be considered as constant [see Eqs. (123)–(125)]. The function $D(\mathbf{p}_1,\mathbf{p}_+)$ is expressed in terms of the momenta in the $[K_S^0\pi^-]$ center-of-mass system defined in the Appendix:

$$D(\mathbf{p}_1,\mathbf{p}_+)=\frac{1}{3}(|\mathbf{p}_1||\mathbf{p}_+|)^2-(\mathbf{p}_1\cdot\mathbf{p}_+)^2. \tag{25}$$

The transition form factor $F^{D^0R_D[\bar{K}^0\pi^-]}(s_-,m_\pi^2)$ follows from Ref. [37] [see their Eq. (10a)], and depends on three distinct functions of the four momentum transfer squared at m_π^2, $k^{D^0K_2^{*-}}(m_\pi^2)$, $b_+^{D^0K_2^{*-}}(m_\pi^2)$ and $b_-^{D^0K_2^{*-}}(m_\pi^2)$, such that

$$F^{D^0R_D[\bar{K}^0\pi^-]}(s_-,m_\pi^2)=k^{D^0K_2^{*-}}(m_\pi^2)+b_+^{D^0K_2^{*-}}(m_\pi^2)(m_{D^0}^2-s_-)+b_-^{D^0K_2^{*-}}(m_\pi^2)m_\pi^2. \tag{26}$$

For the amplitude related to the f_2 meson with mass $m_{f_2}\equiv m_{f_2(1270)}$, one has

$$T^{\rm CF}_{\bar{K}^0[\pi^+\pi^-]_D}(s_0,s_-,s_+)=-\frac{G_F}{2}a_2\Lambda_1\frac{f_{K^0}}{\sqrt{2}}F^{D^0R_D[\pi^+\pi^-]}(s_0,m_{K^0}^2)\times\frac{g_{f_2\pi^+\pi^-}D(\mathbf{p}_2,\mathbf{p}_0)}{m_{f_2}^2-s_0-im_{f_2}\Gamma_{f_2}(s_0)}\equiv T_7, \tag{27}$$

where $g_{f_2\pi^+\pi^-}$ characterizes the strength of the $f_2\to\pi^+\pi^-$ transition [see Eqs. (119) and (120)]. Here, because of the rather large width of the f_2 meson, the total width $\Gamma_{f_2}(s_0)$ depends on the invariant mass squared s_0. The function $D(\mathbf{p}_2,\mathbf{p}_0)$ is given by the same expression as in Eq. (25) replacing $\mathbf{p}_1$ by $\mathbf{p}_2$ and $\mathbf{p}_+$ by $\mathbf{p}_0$, the corresponding momenta and scalar product defined in Eqs. (A4)–(A6). In Eq. (27), the D^0 to f_2 transition form factor, $F^{D^0R_D[\pi^+\pi^-]}(s_0,m_{K^0}^2)$ depends on three distinct functions of the four momentum transfer squared at $m_{K^0}^2$:

$$F^{D^0R_D[\pi^+\pi^-]}(s_0,m_{K^0}^2)=k^{D^0f_2}(m_{K^0}^2)+b_+^{D^0f_2}(m_{K^0}^2)(m_{D^0}^2-s_0)+b_-^{D^0f_2}(m_{K^0}^2)m_{K^0}^2. \tag{28}$$

B. The doubly Cabibbo suppressed amplitudes

To the Cabbibo favored amplitudes of the preceding subsection must now be added the doubly Cabibbo suppressed tree amplitudes which are derived from Eq. (10) in a similar way to that used for the CF amplitudes. For the $[K_S^0\pi^+]_S\pi^-$ amplitude, we have

$$T^{\rm DCS}_{[K^0\pi^+]_S\pi^-}(s_0,s_-,s_+)=\frac{G_F}{2}a_1\Lambda_2(m_{D^0}^2-m_\pi^2)\frac{m_{K^0}^2-m_\pi^2}{s_+}\times F_0^{D^0\pi^-}(s_+)F_0^{K^0\pi^+}(s_+)\equiv T_8, \tag{29}$$

while the $K_S^0[\pi^-\pi^+]_S$ amplitude reads

$$T^{\rm DCS}_{K^0[\pi^-\pi^+]_S}(s_0,s_-,s_+)=\frac{\Lambda_2}{\Lambda_1}T^{\rm CF}_{\bar{K}^0[\pi^+\pi^-]_S}(s_0,s_-,s_+)=\frac{\Lambda_2}{\Lambda_1}T_2. \tag{30}$$

For the $[K_S^0\pi^+]_P\pi^-$ amplitude we obtain

$$T^{\rm DCS}_{[K^0\pi^+]_P\pi^-}(s_0,s_-,s_+)=-\frac{G_F}{2}a_1\Lambda_2\left[s_0-s_-+(m_{D^0}^2-m_\pi^2)\frac{m_{K^0}^2-m_\pi^2}{s_+}\right]\times F_1^{D^0\pi^-}(s_+)F_1^{K^0\pi^+}(s_+)\equiv T_9. \tag{31}$$

For the $K_S^0[\pi^-\pi^+]_P$ amplitude, one has two contributions, associated mainly to the $\rho(770)^0$ and to the $\omega(782)$. They read

$$T^{\rm DCS}_{K^0[\pi^-\pi^+]_P}(s_0,s_-,s_+)=\frac{\Lambda_2}{\Lambda_1}T^{\rm CF}_{\bar{K}^0[\pi^+\pi^-]_P}(s_0,s_-,s_+)=\frac{\Lambda_2}{\Lambda_1}T_4 \tag{32}$$

and

$$T^{\rm DCS}_{K^0[\pi^-\pi^+]_\omega}(s_0,s_-,s_+)=\frac{\Lambda_2}{\Lambda_1}T^{\rm CF}_{\bar{K}^0[\pi^+\pi^-]_\omega}(s_0,s_-,s_+)=\frac{\Lambda_2}{\Lambda_1}T_5, \tag{33}$$

respectively. Associated to the $[K\pi]$ and $[\pi\pi]$ D states, there is only one nonzero amplitude, that related to the f_2 meson,

$$T^{\rm DCS}_{K^0[\pi^-\pi^+]_D}(s_0,s_-,s_+)=\frac{\Lambda_2}{\Lambda_1}T^{\rm CF}_{\bar{K}^0[\pi^+\pi^-]_D}(s_0,s_-,s_+)=\frac{\Lambda_2}{\Lambda_1}T_7. \tag{34}$$

No contribution comes from the $[K\pi]$ D wave since one has $\langle 0|(\bar{u}s)_{V-A}|K_2^{*+}\rangle=0$, so that

$$T^{\rm DCS}_{[K^0\pi^+]_D\pi^-}(s_0,s_-,s_+)\propto T_{10}=0. \tag{35}$$

The expressions of the CF and DCS "emission" amplitudes of the D^0 to pseudoscalar-vector meson decays, given in the Appendix of Ref. [19], agree with our CF [see Eqs. (15), (16), and (23)] and DCS [see Eqs. (31)–(33)] tree amplitudes for the dominant resonance $K^*(892)$, $\rho(770)^0$ and ω part, respectively.

C. The annihilation (W-exchange) Cabibbo favored amplitudes

Let us sketch a systematic derivation for these amplitudes defined in Eq. (11) and illustrated diagrammatically by Fig. 5 (see, e.g., Sec. V C in Ref. [33]). Denoting by $M_1(p_1)$ and $M_2(p_2)$ the quasi-two-meson final state, we may write, in the quasi-two-body factorization, for the CF amplitudes,

$$\langle M_1(p_1)M_2(p_2)|H_{\rm eff}|D^0(p_{D^0})\rangle = \frac{G_F}{\sqrt{2}}a_2\Lambda_1\langle M_1(p_1)M_2(p_2)|(\bar{s}d)_{V-A}|0\rangle\cdot\langle 0|(\bar{u}c)_{V-A}|D^0(p_{D^0})\rangle. \tag{36}$$

The second term in the right-hand side of Eq. (36) corresponds to the annihilation of the D^0 that goes through the W exchange between the $c\bar{u}$ quark pair that builds the D^0 (see Ref. [33]). In Eq. (36) the possible quasi-two-meson pairs are [see Eq. (11)]

$$M_1(p_0+p_-)\equiv[\bar{K}^0(p_0)\pi^-(p_-)]_L,\quad M_2(p_+)\equiv\pi^+(p_+), \tag{37}$$

$$M_1(p_++p_-)\equiv[\pi^+(p_+)\pi^-(p_-)]_L,\quad M_2(p_0)\equiv\bar{K}^0(p_0). \tag{38}$$

The meson pairs are assumed to originate from a pair of quarks: a $s\bar{u}$ pair in the first case and a $d\bar{d}$ one in the second. For the D^0 decay constant, f_{D^0}, one takes [the phase is chosen in accordance with the choice made in Eq. (A.3) of Ref. [27]]

$$\langle 0|(\bar{u}c)_{V-A}|D^0(p_{D^0})\rangle = -if_{D^0}p_{D^0}. \tag{39}$$

Thus, all annihilation amplitudes will be proportional to the D^0 decay constant f_{D^0}. The form factor $\langle M_1(p_1)M_2(p_2)|(\bar{s}d)_{V-A}|0\rangle$ is evaluated in terms of the transition form factors between the pseudoscalar $M_2(-p_2)$ and the meson pair $[m_1(p_3)m_2(p_4)]_L$ in the scalar, the vector or the tensor state, with respective four momenta p_3 and p_4. We introduce the hypothesis that the transitions of the pseudoscalar meson $M_2(-p_2)$ to the $[m_1(p_3)m_2(p_4)]_L$ states go through intermediate resonances $M_1(p_1)$ where the four momentum p_1 fulfills the energy-momentum conservation relation $p_1=p_3+p_4$; these intermediate resonances then decay into the $[m_1(p_3),m_2(p_4)]$ pairs. In the case of Eq. (37), one identifies $m_1(p_3)$ with the $\bar{K}^0$ meson with four momentum p_0 and $m_2(p_4)$ with the π^- meson with four momentum p_- whereas, in the case of Eq. (38) one identifies $m_1(p_3)$ with the π^+ meson with four momentum p_+ and $m_2(p_4)$ with the π^- meson with four momentum p_-. The resonance decays are described by vertex functions $G_{R_L[m_1m_2]}(p_1^2)$ modeled assuming them to be proportional to the scalar $R_S[m_1m_2]$ or vector $R_P[m_1m_2]$ form factor for the S and P amplitudes or to a relativistic Breit-Wigner function for the $R_D[m_1m_2]$ states. The model thus yields the following contributions.

For $[m_1m_2]_S$ waves

$$\begin{aligned}\langle M_1(p_1)M_2(p_2)|(\bar{s}d)_{V-A}|0\rangle &= G_{R_S[m_1m_2]}(s_{34})\langle R_S[m_1(p_3)m_2(p_4)]|(\bar{s}d)_{V-A}|M_2(-p_2)\rangle\\ &= -iG_{R_S[m_1m_2]}(s_{34})\Bigg\{\left[-p_2+p_3+p_4+\frac{p_2^2-(p_3+p_4)^2}{m_{D^0}^2}p_{D^0}\right]\\ &\quad\times F_1^{M_2R_S[m_1m_2]}(m_{D^0}^2)-\frac{p_2^2-(p_3+p_4)^2}{m_{D^0}^2}p_{D^0}F_0^{M_2R_S[m_1m_2]}(m_{D^0}^2)\Bigg\},\end{aligned} \tag{40}$$

where $F_0^{M_2R_S[m_1m_2]}(m_{D^0}^2)$ and $F_1^{M_2R_S[m_1m_2]}(m_{D^0}^2)$ denote the $M_2R_S[m_1m_2]$ scalar and vector form factors. The vertex function $G_{R_S[m_1m_2]}(s_{34})$ is modeled according to

$$G_{R_S[m_1m_2]}(s_{34})=\chi_{R_S[m_1m_2]}F_0^{m_1m_2}(s_{34}),\qquad \text{with}\quad s_{34}=p_1^2=(p_3+p_4)^2, \tag{41}$$

$F_0^{m_1m_2}(s_{34})$ being the $[m_1m_2]$ scalar form factor and $\chi_{R_S[m_1m_2]}$ characterizing the strength of the S-state form factor contribution as discussed in Sec. II A. With $\chi_{R_S[\bar{K}^0\pi^-]}\equiv\chi_1$ [see Eq. (13)] the CF $[\bar{K}^0(p^0)\pi^-(p_-)]_S\pi^+(p_+)$ annihilation amplitude is

$$\begin{aligned}A^{\rm CF}_{[\bar{K}^0\pi^-]_S\pi^+}(s_0,s_-,s_+) &= -\frac{G_F}{2}a_2\Lambda_1\chi_1(m_\pi^2-s_-)f_{D^0}\\ &\quad\times F_0^{\pi^+R_S[\bar{K}^0\pi^-]}(m_{D^0}^2)F_0^{\bar{K}^0\pi^-}(s_-)\\ &\equiv A_1.\end{aligned} \tag{42}$$

For the $[\pi^+(p_+)\pi^-(p_-)]_S$ pair, we have, with $\chi_{R_S[\pi^+\pi^-]}\equiv\chi_2$ [see Eq. (14)]

$$\begin{aligned}A^{\rm CF}_{\bar{K}^0[\pi^+\pi^-]_S}(s_0,s_-,s_+) &= -\frac{G_F}{2}a_2\Lambda_1\chi_2(m_{K^0}^2-s_0)f_{D^0}\\ &\quad\times F_0^{\bar{K}^0R_S[\pi^+\pi^-]}(m_{D^0}^2)F_0^{\pi^+\pi^-}(s_0)\\ &\equiv A_2.\end{aligned} \tag{43}$$

Since the D^0 mass is larger than the masses of the two-meson thresholds $m_\pi+m_{K_0^*(800)}$ and $m_{\bar{K}^0}+m_{f_0(500)}$, the transition form factors $F_0^{\pi^+R_S[\bar{K}^0\pi^-]}(m_{D^0}^2)$ and $F_0^{\bar{K}^0R_S[\pi^+\pi^-]}(m_{D^0}^2)$ appearing in these equations are unknown complex parameters to be fitted.

For the $[m_1m_2]_P$ wave contributions, denoting for simplicity the vector meson resonances as

$$V_R \equiv R_P[m_1 m_2],$$

we may write

$$\langle [m_1(p_3)m_2(p_4)]_P M_2(p_2)|(\bar{d}s)_{V-A}|0\rangle = G_{V_R}(p_1^2)\epsilon\cdot(p_3-p_4)\langle V_R(p_1^2)|(\bar{s}d)_{V-A}|M_2(-p_2)\rangle, \tag{44}$$

ϵ being the polarization of the vector resonance and G_{V_R} the V_R decay vertex function. One has [33]

$$\langle V_R(p_1^2)|(\bar{s}d)_{V-A}|M_2(-p_2)\rangle = -i\frac{2m_{V_R}(\epsilon^*\cdot p_2)}{p_{D^0}^2}p_{D^0}A_0^{M_2V_R}(m_{D^0}^2) + \text{“other terms”}. \tag{45}$$

Here $p_{D^0} = p_1 + p_2$. The “other terms” do not contribute when multiplying the matrix element (45) by that of Eq. (39). The P states being characterized by dominant resonances, one writes

$$G_{V_R}(p_1^2) = \frac{1}{m_{V_R}f_{V_R}}F_1^{m_1m_2}(p_1^2),$$

where f_{V_R} is the V_R decay constant. One thus arrives at the following expressions:

$$A^{\rm CF}_{[\bar{K}^0\pi^-]_P\pi^+}(s_0,s_-,s_+) = -\frac{G_F}{2}a_2\Lambda_1\frac{f_{D^0}}{f_{K^{*-}}}\left[s_0 - s_+\frac{(m_{D^0}^2-m_\pi^2)(m_{K^0}^2-m_\pi^2)}{s_-}\right] \times A_0^{\pi^+R_P[\bar{K}^0\pi^-]}(m_{D^0}^2)F_1^{\bar{K}^0\pi^-}(s_-) \equiv A_3, \tag{46}$$

and

$$A^{\rm CF}_{\bar{K}^0[\pi^+\pi^-]_P}(s_0,s_-,s_+) = \frac{G_F}{2}a_2\Lambda_1\frac{f_{D^0}}{f_\rho}(s_- - s_+)A_0^{\bar{K}^0R_P[\pi^+\pi^-]}(m_{D^0}^2)F_1^{\pi^+\pi^-}(s_0) \equiv A_4, \tag{47}$$

and, if the $[\pi^-\pi^+]_P$ originates from the ω resonance,

$$A^{\rm CF}_{\bar{K}^0[\pi^+\pi^-]_\omega}(s_0,s_-,s_+) = -\frac{G_F}{2}a_2\Lambda_1\frac{f_{D^0}}{\sqrt{2}}m_\omega(s_- - s_+)\frac{g_{\omega\pi\pi}A_0^{\bar{K}^0[\pi^+\pi^-]_\omega}(m_{D^0}^2)}{m_\omega^2 - s_0 - im_\omega\Gamma_\omega} \equiv A_5. \tag{48}$$

Since we are in the $\bar{K}^0V_R$ scattering region, the values of the form factors $A_0^{\bar{K}^0R_P[\pi^+\pi^-]}(m_{D^0}^2)$ and $A_0^{\bar{K}^0[\pi+\pi^-]_\omega}(m_{D^0}^2)$ are complex numbers.

Finally, for the $[m_1m_2]_D$-wave contributions, denoting for simplicity the tensor meson resonances as

$$T_R \equiv T_R[m_1m_2]$$

and the polarization tensor of the D-wave resonance as $\epsilon_{\alpha\beta}(\lambda)$, λ being the spin projection, one can write

$$\langle [m_1(p_3)m_2(p_4)]_D M_2(p_2)|(\bar{s}d)_{V-A}|0\rangle = G_{T_R}(p_1^2)\sum_{\lambda=-2}^{\lambda=+2}\epsilon_{\alpha\beta}(\lambda)p_3^\alpha p_4^\beta\langle T_R^\lambda(p_1^2)M_2(-p_2)|(\bar{s}d)_{V-A}|0\rangle. \tag{49}$$

Reformulating the matrix element for the M_2T_R to vacuum transition

$$-if_{D^0}p_{D^0}\cdot\langle T_R^\lambda(p_1^2)M_2(p_2)|(\bar{s}d)_{V-A}|0\rangle = f_{D^0}F^{M_2T_R}(p_1^2,m_{D^0}^2)\epsilon_{\mu\nu}^*(\lambda)p_2^\nu p_2^\mu, \tag{50}$$

where (see Ref. [37])

$$-iF^{M_2T_R}(p_1^2,m_{D^0}^2) = k^{M_2T_R}(m_{D^0}^2) + b_+^{M_2T_R}(m_{D^0}^2)(m_{M_2}^2 - p_1^2) + b_-^{M_2T_R}(m_{D^0}^2)m_{D^0}^2. \tag{51}$$

Here, $k^{M_2T_R}$, $b_+^{M_2T_R}$ and $b_-^{M_2T_R}$ are complex transition form factors since $m_{D^0}^2 > (m_{M_2}+m_{T_R})^2$. Assuming then, for these cases, Breit-Wigner representations of the resonance vertex functions $G_{T_R}(p_1^2)$ and summing over the spin projections λ, one arrives at the following expressions:

$$A^{\rm CF}_{[\bar{K}^0\pi^-]_D\pi^+}(s_0,s_-,s_+) = \frac{G_F}{2}a_2\Lambda_1 f_{D^0}F^{R_D[\bar{K}^0\pi^-]\pi^+}(s_-,m_{D^0}^2) \times g_{K_2^{*-}K_S^0\pi^-}\frac{D(\mathbf{p}_1,\mathbf{p}_+)}{m_{K_2^*}^2 - s_- - im_{K_2^*}\Gamma_{K_2^*}} \equiv A_6, \tag{52}$$

$$A^{\rm CF}_{\bar{K}^0[\pi^+\pi^-]_D}(s_0,s_-,s_+) = \frac{G_F}{2}a_2\Lambda_1\frac{f_{D^0}}{\sqrt{2}}F^{\bar{K}^0R_D[\pi^+\pi^-]}(s_0,m_{D^0}^2) \times g_{f_2\pi^+\pi^-}\frac{D(\mathbf{p}_2,\mathbf{p}_0)}{m_{f_2}^2 - s_0 - im_{f_2}\Gamma_{f_2}(s_0)} \equiv A_7, \tag{53}$$

where the expressions of $g_{K_2^{*-}K_S^0\pi^-}$, $g_{f_2\pi^+\pi^-}$ and of the resonance widths are discussed in Sec. IV.

D. The annihilation (W-exchange) doubly Cabibbo suppressed amplitudes

One has to evaluate the corresponding Cabbibo suppressed amplitudes. One obtains for the $[K_S^0\pi^+]_S\pi^-$ amplitudes

$$A^{\rm DCS}_{[K^0\pi^+]_S\pi^-}(s_0,s_-,s_+) = -\frac{G_F}{2}a_2\Lambda_2\chi_1(m_\pi^2-s_+)f_{D^0}F_0^{\pi^-R_S[K^0\pi^+]}(m^2_{D^0})F_0^{K^0\pi^+}(s_+) \equiv A_8, \quad (54)$$

and

$$A^{\rm DCS}_{K^0[\pi^-\pi^+]_S}(s_0,s_-,s_+) = A^{\rm CF}_{\bar K^0[\pi^+\pi^-]_S}(s_0,s_-,s_+) = \frac{\Lambda_2}{\Lambda_1}A_2, \quad (55)$$

for the $K^0_S[\pi^-\pi^+]_S$ amplitude, having assumed the charge symmetry relation for the form factors

$$F_0^{K^0R_S[\pi^-\pi^+]}(m^2_{D^0}) = F_0^{\bar K^0R_S[\pi^+\pi^-]}(m^2_{D^0}). \quad (56)$$

For the $[K^0_S\pi^+]_P\pi^-$ amplitudes, one has with $K^{*+}\equiv K^{*+}(892)$ [compare with Eq. (46)]

$$A^{\rm DCS}_{[K^0\pi^+]_P\pi^-}(s_0,s_-,s_+) = -\frac{G_F}{2}a_2\Lambda_2\frac{f_{D^0}}{f_{K^{*+}}}\left[s_0-s_-+\frac{(m^2_{D^0}-m^2_\pi)(m^2_{K^0}-m^2_\pi)}{s_+}\right] \times A_0^{R_P[K^0\pi^+]\pi^-}(m^2_{D^0})F_1^{K^0\pi^+}(s_+) \equiv A_9, \quad (57)$$

while for the $K^0_S[\pi^-\pi^+]_P$ amplitudes, assuming the charge symmetry relations

$$A_0^{K^0R_P[\pi^-\pi^+]}(m^2_{D^0}) = A_0^{\bar K^0R_P[\pi^+\pi^-]}(m^2_{D^0}) \quad (58)$$

$$A_0^{K^0[\pi^-\pi^+]_\omega}(m^2_{D^0}) = A_0^{\bar K^0[\pi^+\pi^-]_\omega}(m^2_{D^0}), \quad (59)$$

one obtains respectively

$$A^{\rm DCS}_{K^0[\pi^-\pi^+]_P}(s_0,s_-,s_+) = \frac{\Lambda_2}{\Lambda_1}A^{\rm CF}_{\bar K^0[\pi^+\pi^-]_P}(s_0,s_-,s_+) = \frac{\Lambda_2}{\Lambda_1}A_4, \quad (60)$$

$$A^{\rm DCS}_{K^0[\pi^-\pi^+]_\omega}(s_0,s_-,s_+) = \frac{\Lambda_2}{\Lambda_1}A^{\rm CF}_{\bar K^0[\pi^+\pi^-]_\omega}(s_0,s_-,s_+) = \frac{\Lambda_2}{\Lambda_1}A_5. \quad (61)$$

Finally, the $[K^0_S\pi^+]_D\pi^-$ amplitude reads

$$A^{\rm DCS}_{[K^0\pi^+]_D\pi^-}(s_0,s_-,s_+) = \frac{G_F}{2}a_2\Lambda_2 f_{D^0}F^{R_D[K^0\pi^+]\pi^-}(s_+,m^2_{D^0}) \times g_{K_2^{*+}K^0_S\pi^+}\frac{D(\mathbf{p}_3,\mathbf{p}_-)}{m^2_{K_2^*}-s_+-im_{K_2^*}\Gamma_{K_2^*}} \equiv A_{10}, \quad (62)$$

where $\mathbf{p}_3$ and $\mathbf{p}_-$ are defined in the Appendix, and with the charge symmetry relation

$$F^{K^0R_D[\pi^-\pi^+]}(s_0,m^2_{D^0}) = F^{\bar K^0R_D[\pi^+\pi^-]}(s_0,m^2_{D^0}), \quad (63)$$

the $K^0_S[\pi^-\pi^+]_D$ amplitude is

$$A^{\rm DCS}_{K^0[\pi^-\pi^+]_D}(s_0,s_-,s_+) = \frac{\Lambda_2}{\Lambda_1}A^{\rm CF}_{\bar K^0[\pi^+\pi^-]_D}(s_0,s_-,s_+) = \frac{\Lambda_2}{\Lambda_1}A_7. \quad (64)$$

To summarize, of the 28 amplitudes describing the $D^0\to K^0_S\pi^+\pi^-$ decays, only 20 are independent among which one, $T^{\rm DCS}_{[K^0\pi^+]_D\pi^-}(s_0,s_-,s_+)$ or T_{10}, is zero [Eq. (35)].

III. QUASI-TWO-BODY CHANNEL AMPLITUDES AND BRANCHING FRACTIONS

This section is devoted to the construction of amplitudes suited for numerical computations. This aim leads us to build specific combinations out of the amplitudes formally derived in the preceding section. The full decay amplitude given in Eq. (5) can be written in the quasi two-body-factorization approximation as a superposition of ten partial amplitudes $\mathcal{M}_i$ which are each made of a tree $\mathcal{T}_i$ and of an annihilation (W-exchange) $\mathcal{A}_i$ contribution:

$$\mathcal{M}_F \equiv \sum_{i=1}^{10}\mathcal{M}_i \equiv \sum_{i=1}^{10}(\mathcal{T}_i+\mathcal{A}_i). \quad (65)$$

A. Amplitudes recombined

From Eqs. (6), (11), (13), and (42), the summed $[K^0_S\pi^-]_S\pi^+$ CF amplitudes read

$$\mathcal{M}_1 \equiv \mathcal{T}_1+\mathcal{A}_1 = T_1+A_1 = -\frac{G_F}{2}\Lambda_1\chi_1F_0^{\bar K^0\pi^-}(s_-) \times [a_1(m^2_{D^0}-s_-)f_\pi F_0^{D^0R_S[\bar K^0\pi^-]}(m^2_\pi) + a_2(m^2_\pi-s_-)f_{D^0}F_0^{R_S[\bar K^0\pi^-]\pi^+}(m^2_{D^0})]. \quad (66)$$

Recombining the tree amplitudes defined in Eqs. (6) and (10) and given by Eqs. (14) and (30), and the annihilation amplitudes defined in Eqs. (11) and (12), and given by Eqs. (43) and (55), yields the complete $K^0_S[\pi^+\pi^-]_S$ amplitude,

$$\mathcal{M}_2 \equiv \mathcal{T}_2+\mathcal{A}_2 = \left(1+\frac{\Lambda_2}{\Lambda_1}\right)(T_2+A_2) = -\frac{G_F}{2}a_2(\Lambda_1+\Lambda_2)\chi_2F_0^{\pi^+\pi^-}(s_0) \times [(m^2_{D^0}-s_0)f_{K^0}F_0^{D^0R_S[\pi^+\pi^-]}(m^2_{K^0}) + (m^2_{K^0}-s_0)f_{D^0}F_0^{\bar K^0R_S[\pi^+\pi^-]}(m^2_{D^0})]. \quad (67)$$

For the P states, the summed $[K^0_S\pi^-]_P\pi^+$ CF amplitudes from Eqs. (6), (11), (15), and (46) yield

$$\mathcal{M}_3 \equiv \mathcal{T}_3 + \mathcal{A}_3 = T_3 + A_3 = \frac{G_F}{2}\Lambda_1\left[s_0 - s_+ + \frac{(m_{D^0}^2 - m_\pi^2)(m_{\bar{K}^0}^2 - m_\pi^2)}{s_-}\right] F_1^{\bar{K}^0\pi^-}(s_-)$$
$$\times\left[a_1\frac{f_\pi}{f_{K^{*-}}}A_0^{D^0R_P[\bar{K}^0\pi^-]}(m_\pi^2) - a_2\frac{f_{D^0}}{f_{K^{*-}}}A_0^{\pi^+R_P[\bar{K}^0\pi^-]}(m_{D^0}^2)\right]. \quad (68)$$

As in the case of the $K_S^0[\pi^+\pi^-]_S$ channel, one aggregates the four CF and DCS amplitudes given in Eqs. (16), (32), (47), and (60) to obtain the complete $K_S^0[\pi^+\pi^-]_P$ amplitude,

$$\mathcal{M}_4 \equiv \mathcal{T}_4 + \mathcal{A}_4 = \left(1 + \frac{\Lambda_2}{\Lambda_1}\right)(T_4 + A_4)$$
$$= \frac{G_F}{2}a_2(\Lambda_1 + \Lambda_2)\frac{1}{f_\rho}(s_- - s_+)F_1^{\pi^+\pi^-}(s_0)[f_{K^0}A_0^{D^0R_P[\pi^+\pi^-]}(m_{K^0}^2) + f_{D^0}A_0^{\bar{K}^0R_P[\pi^+\pi^-]}(m_{D^0}^2)]. \quad (69)$$

The combination,

$$f_{K^0}A_0^{D^0R_P[\pi^+\pi^-]}(m_{K^0}^2) + f_{D^0}A_0^{\bar{K}^0R_P[\pi^+\pi^-]}(m_{D^0}^2), \quad (70)$$

will be treated as a single real parameter (see Sec. III B).

The $K_S^0[\pi^+\pi^-]_\omega$ amplitude results from Eqs. (23), (33), (48), and (61):

$$\mathcal{M}_5 \equiv \mathcal{T}_5 + \mathcal{A}_5 = \left(1 + \frac{\Lambda_2}{\Lambda_1}\right)(T_5 + A_5)$$
$$= \frac{G_F}{2}(\Lambda_1 + \Lambda_2)\frac{a_2}{\sqrt{2}}m_\omega(s_- - s_+)[f_{K^0}A_0^{D^0\omega}(m_{K^0}^2) - f_{D^0}A_0^{\bar{K}^0[\pi^+\pi^-]_\omega}(m_{D^0}^2)]\frac{g_{\omega\pi\pi}}{m_\omega^2 - s_0 - im_\omega\Gamma_\omega}. \quad (71)$$

The $[K_S^0\pi^-]_D\pi^+$ amplitude, which arises from Eqs. (6), (11), (24), (35), and (52), reads

$$\mathcal{M}_6 \equiv \mathcal{T}_6 + \mathcal{A}_6 = T_6 + A_6 = \frac{G_F}{2}\Lambda_1 g_{K_2^{*-}K_S^0\pi^-}B_{K_2^*}(s_+, s_-)[-a_1f_\pi F^{D^0R_D[\bar{K}^0\pi^-]}(s_-, m_\pi^2) + a_2f_{D^0}F^{R_D[\bar{K}^0\pi^-]\pi^+}(s_-, m_{D^0}^2)], \quad (72)$$

where

$$B_{K_2^*}(s_+, s_-) = \frac{D(\mathbf{p}_1, \mathbf{p}_+)}{m_{K_2^*}^2 - s_- - im_{K_2^*}\Gamma_{K_2^*}}. \quad (73)$$

Using

$$F^{D^0R_D[\bar{K}^0\pi^-]}(s_-, m_\pi^2) = D_1 + E_1(m_{D^0}^2 - s_-) \quad (74)$$

and

$$F^{R_D[\bar{K}^0\pi^-]\pi^+}(s_-, m_{D^0}^2) = d_1 + e_1(m_\pi^2 - s_-), \quad (75)$$

where D_1 and E_1 are real coefficients, related to the form factors in Eq. (26) by

$$D_1 = k^{D^0K_2^{*-}}(m_\pi^2) + b_-^{D^0K_2^{*-}}(m_\pi^2)m_\pi^2 \qquad \text{and}$$
$$E_1 = b_+^{D^0K_2^{*-}}(m_\pi^2)$$

while d_1 and e_1, related to the form factors in Eq. (51) by

$$d_1 = k^{K_2^{*-}\pi^+}(m_{D^0}^2) + b_-^{K_2^{*-}\pi^+}(m_{D^0}^2)m_{D^0}^2 \qquad \text{and}$$
$$e_1 = b_+^{K_2^{*-}\pi^+}(m_{D^0}^2)$$

are complex. One finally obtains

$$\mathcal{M}_6 = \frac{G_F}{2}\Lambda_1 g_{K_2^{*-}K_S^0\pi^-}\left(q_6 m_{K_2^*} + \frac{s_6}{m_{K_2^*}}s_-\right)B_{K_2^*}(s_+, s_-) \quad (76)$$

with

$$q_6 m_{K_2^*} = -a_1f_\pi(D_1 + E_1m_{D^0}^2) + a_2f_{D^0}(d_1 + e_1m_\pi^2), \quad (77)$$

$$\frac{s_6}{m_{K_2^*}} = a_1f_\pi E_1 - a_2f_{D^0}e_1. \quad (78)$$

The unknown complex parameters q_6 and s_6 will be fitted.

For the $K^0_S[\pi^+\pi^-]_D$ amplitude dominated by the f_2 meson, we have, from Eqs. (6), (10)–(12), (27), (34), (53), and (64),

$$\begin{aligned}\mathcal{M}_7 &\equiv \mathcal{T}_7 + \mathcal{A}_7 = \left(1+\frac{\Lambda_2}{\Lambda_1}\right)(T_7 + A_7)\\ &= \frac{G_F}{2\sqrt{2}} a_2(\Lambda_1+\Lambda_2) g_{f_2\pi^+\pi^-}\\ &\quad\times[-f_{K^0}F^{D^0R_D[\pi^+\pi^-]}(s_0, m^2_{K^0})\\ &\quad + f_{D^0}F^{\bar{K}^0R_D[\pi^+\pi^-]}(s_0, m^2_{D^0})]B_{f_2}(s_+, s_0)\end{aligned} \tag{79}$$

with

$$B_{f_2}(s_+, s_0) = \frac{D(\mathbf{p}_2, \mathbf{p}_0)}{m^2_{f_2} - s_0 - i m_{f_2}\Gamma_{f_2}(s_0)}. \tag{80}$$

It is reexpressed as

$$\begin{aligned}\mathcal{M}_7 &= \frac{G_F}{2\sqrt{2}}(\Lambda_1+\Lambda_2) g_{f_2\pi^+\pi^-}\left(q_7 m_{f2} + \frac{s_7}{m_{f2}} s_0\right)\\ &\quad\times B_{f_2}(s_+, s_0),\end{aligned} \tag{81}$$

with

$$q_7 m_{f2} = a_2[-f_{K^0}(D_2 + E_2 m^2_{D^0}) + f_{D^0}(d_2 + e_2 m^2_{K^0})] \tag{82}$$

$$\frac{s_7}{m_{f2}} = a_2(f_{K^0}E_2 - f_{D^0}e_2). \tag{83}$$

As for the $[K^0_S\pi^-]_D\pi^+$ amplitude, the coefficients D_2, E_2 are real but related to the form factors in Eq. (28) by

$$\begin{aligned}D_2 &= k^{D^0 f_2}(m^2_{K^0}) + b^{D^0 f_2}_-(m^2_{K^0}) m^2_{K^0} \qquad \text{and}\\ E_2 &= b^{D^0 f_2}_+(m^2_{K^0}),\end{aligned}$$

while d_2 and e_2, arising from the form factors of Eq. (51), are complex. As q_6 and s_6, q_7 and s_7 are unknown parameters that will be fitted.

The DCS $[K^0_S\pi^+]_S\pi^-$ amplitude results from Eqs. (10), (12), (29), and (54) and reads

$$\begin{aligned}\mathcal{M}_8 &\equiv \mathcal{T}_8 + \mathcal{A}_8\\ &= z_8(T_8 + A_8)\\ &= \frac{G_F}{2}\Lambda_2 z_8\left[a_1(m^2_{D^0} - m^2_\pi)\frac{m^2_{K^0} - m^2_\pi}{s_+} F_0^{D^0\pi^-}(s_+)\right.\\ &\quad\left. - a_2\chi_1 f_{D^0}(m^2_\pi - s_+) F_0^{\pi^- R_S[K^0\pi^+]}(m^2_{D^0})\right] F_0^{K^0\pi^+}(s_+)\end{aligned} \tag{84}$$

and the DCS $[K^0_S\pi^+]_P\pi^-$ amplitude results from Eqs. (10), (12), (31), and (57):

$$\begin{aligned}\mathcal{M}_9 &\equiv \mathcal{T}_9 + \mathcal{A}_9\\ &= z_9(T_9 + A_9)\\ &= -\frac{G_F}{2}\Lambda_2 z_9\left[a_1 F_1^{D^0\pi^-}(s_+)\right.\\ &\quad\left. + a_2\frac{f_{D^0}}{f_{K^{*+}}} A_0^{R_P[K^0\pi^+]\pi^-}(m^2_{D^0})\right]\\ &\quad\times\left[s_0 - s_- + \frac{(m^2_{D^0} - m^2_\pi)(m^2_{K^0} - m^2_\pi)}{s_+}\right] F_1^{K^0\pi^+}(s_+).\end{aligned} \tag{85}$$

The unknown multiplicative complex constants z_8 and z_9, appearing in Eqs. (84) and (85), are introduced to allow some charge independence violation in the $[K\pi]_S\pi$ and $[K\pi]_P\pi$ amplitudes, as can be seen comparing, on the one hand, amplitudes $\mathcal{M}_1$ in Eq. (66) and $\mathcal{M}_8$ in Eq. (84) and, on the other hand, amplitudes $\mathcal{M}_3$ in Eq. (68) and $\mathcal{M}_9$ in Eq. (85). They will be fitted. In the calculations that follow, we assume that the $[K\pi]_{S,P}$ form factors fulfill the relation

$$F^{K^0\pi^+}_{(0,1)}(s) \equiv F^{\bar{K}^0\pi^-}_{(0,1)}(s). \tag{86}$$

Finally, from Eq. (62), the DCS annihilation $[K\pi]_D\pi$ amplitude is $\mathcal{M}_{10} \equiv A_{10}$. In analogy with the amplitudes $\mathcal{M}_6$ and $\mathcal{M}_7$, we introduce the parametrization

$$a_2 f_{D^0} F^{R_D[K^0\pi^+]\pi^-}(s_+, m^2_{D^0}) = q_{10} m_{K^*_2} + \frac{s_{10}}{m_{K^*_2}} s_+, \tag{87}$$

where the unknown coefficients q_{10} and s_{10}, related to the transition form factors in Eq. (51), are free complex parameters that will be fitted. We calculate practically

$$\mathcal{M}_{10} = \frac{G_F}{2}\Lambda_2\left(q_{10} m_{K^*_2} + \frac{s_{10}}{m_{K^*_2}} s_+\right)\frac{g_{K^{*+}_2 K^0\pi^+} D(p_3, p_-)}{m^2_{K^*_2} - s_+ - i m_{K^*_2}\Gamma_{K^*_2}}. \tag{88}$$

To summarize this subsection, the recombined amplitudes used in our calculations are given in Table I (a similar table can be established for the conjugate $\bar{D}^0$ decays).

B. On branching fractions

The differential branching fraction or the Dalitz plot density distribution is defined as

$$\frac{d^2\mathrm{Br}}{ds_- ds_+} = \frac{|\mathcal{M}|^2}{32(2\pi)^3 m^3_{D^0}\Gamma_{D^0}}, \tag{89}$$

where Γ_{D^0} is the D^0 width. The total branching fraction for the D^0 decay into $K^0_S\pi^+\pi^-$ is obtained by integration of the differential branching fraction over the Dalitz diagram surface. One can also obtain one-dimensional densities

TABLE I. Summary of the Cabibbo favored, CF, and doubly Cabibbo suppressed, DCS, amplitudes associated to the different quasi-two-body channels. For each channel, the dominant resonances are listed in column 3 and the total amplitudes, $\mathcal{M}_i$, $i = 1, 10$, are the sum of the CF and DCS amplitudes. The tree and annihilation amplitudes are denoted T_i and A_i, respectively.

Amplitude	Quasi-two-body channel	Dominant resonances	CF amplitudes	DCS amplitudes
$\mathcal{M}_1$	$[K^0_S\pi^-]_S\pi^+$	$K^*_0(800)^-$, $K^*_0(1430)^-$	$T_1 + A_1$	
$\mathcal{M}_2$	$K^0_S[\pi^+\pi^-]_S$	$f_0(500)$, $f_0(980)$, $f_0(1400)$	$T_2 + A_2$	$\frac{\Lambda_2}{\Lambda_1}(T_2 + A_2)$
$\mathcal{M}_3$	$[K^0_S\pi^-]_P\pi^+$	$K^*(892)^-$	$T_3 + A_3$	
$\mathcal{M}_4$	$K^0_S[\pi^+\pi^-]_P$	$\rho(770)$	$T_4 + A_4$	$\frac{\Lambda_2}{\Lambda_1}(T_4 + A_4)$
$\mathcal{M}_5$	$K^0_S[\pi^+\pi^-]_\omega$	$\omega(782)$	$T_5 + A_5$	$\frac{\Lambda_2}{\Lambda_1}(T_5 + A_5)$
$\mathcal{M}_6$	$[K^0_S\pi^-]_D\pi^+$	$K^*_2(1430)^-$	$T_6 + A_6$	
$\mathcal{M}_7$	$K^0_S[\pi^+\pi^-]_D$	$f_2(1270)$	$T_7 + A_7$	$\frac{\Lambda_2}{\Lambda_1}(T_7 + A_7)$
$\mathcal{M}_8$	$[K^0_S\pi^+]_S\pi^-$	$K^*_0(800)^+$, $K^*_0(1430)^+$		$z_8(T_8 + A_8)$
$\mathcal{M}_9$	$[K^0_S\pi^+]_P\pi^-$	$K^*(892)^+$		$z_9(T_9 + A_9)$
$\mathcal{M}_{10}$	$[K^0_S\pi^+]_D\pi^-$	$K^*_2(1430)^+$		A_{10}

by integration over one variable s, for example the s_- distribution reads

$$\frac{d\mathrm{Br}}{ds_-} = \int_{(m_\pi + m_{K^0})^2}^{(m_{D^0} - m_\pi)^2} \frac{d^2\mathrm{Br}}{ds_- ds_+} ds_+. \tag{90}$$

We infer from Eq. (89) that it is not possible to calculate all the phases of the amplitudes $\mathcal{M}_i$ by knowing the differential branching fraction distribution only. Out of the ten phases, one phase cannot be determined. Let us call this particular phase ϕ_4 and define the modified partial amplitudes $\tilde{\mathcal{M}}_i$ as follows:

$$\tilde{\mathcal{M}}_i = e^{-i\phi_4}\mathcal{M}_i. \tag{91}$$

The phase ϕ_4 is taken equal to the phase of the constant coefficient of the amplitude $\mathcal{M}_4$ defined in Eq. (69). By making this choice we proceed in the same way as in the isobar model analyses of Refs. [1,2,10]. Our basic amplitudes, which will be determined from the fit to the Dalitz plot density distributions, are the $\tilde{\mathcal{M}}_i$ and $\mathcal{T}_i$ amplitudes.

The branching fraction distributions corresponding to the amplitudes $\mathcal{M}_i$ are defined as

$$\frac{d^2\mathrm{Br}_i}{ds_- ds_+} = \frac{|\mathcal{M}_i|^2}{32(2\pi)^3 m^3_{D^0}\Gamma_{D^0}}. \tag{92}$$

If one replaces $\mathcal{M}_i$ by $\tilde{\mathcal{M}}_i$ then the above branching fractions remain unchanged. It is instructive to define separately the branching fractions corresponding to different tree and annihilation components i of the decay amplitudes,

$$\frac{d^2\mathrm{Br}^{\mathrm{tree}}_i}{ds_- ds_+} = \frac{|\mathcal{T}_i|^2}{32(2\pi)^3 m^3_{D^0}\Gamma_{D^0}}, \tag{93}$$

and

$$\frac{d^2\mathrm{Br}^{\mathrm{ann}}_i}{ds_- ds_+} = \frac{|\mathcal{A}_i|^2}{32(2\pi)^3 m^3_{D^0}\Gamma_{D^0}} = \frac{|e^{i\phi_4}\tilde{\mathcal{M}}_i - \mathcal{T}_i|^2}{32(2\pi)^3 m^3_{D^0}\Gamma_{D^0}}, \tag{94}$$

since from Eqs. (65) and (91) one has

$$\mathcal{A}_i = e^{i\phi_4}\tilde{\mathcal{M}}_i - \mathcal{T}_i. \tag{95}$$

While the branching fractions $d^2\mathrm{Br}_i/ds_- ds_+$ and the tree branching fractions $d^2\mathrm{Br}^{\mathrm{tree}}_i/ds_- ds_+$ can be directly calculated from the fitted amplitudes, the annihilation branching fractions $d^2\mathrm{Br}^{\mathrm{ann}}_i/ds_- ds_+$ cannot be evaluated since the phase ϕ_4 is in general unknown. From Eq. (95) we can, however, obtain the following inequality:

$$|\tilde{\mathcal{M}}_i|^2 + |\mathcal{T}_i|^2 - 2|\tilde{\mathcal{M}}_i||\mathcal{T}_i| \le |\mathcal{A}_i|^2 \le |\tilde{\mathcal{M}}_i|^2 + |\mathcal{T}_i|^2 + 2|\tilde{\mathcal{M}}_i||\mathcal{T}_i| \tag{96}$$

from which the lower and upper limits of the annihilation branching fractions can be calculated. For example, the lower limits of the integrated annihilation branching fractions are given by

$$\mathrm{Br}^{\mathrm{ann,low}}_i = \mathrm{Br}_i + \mathrm{Br}^{\mathrm{tree}}_i - 2\iint ds_- ds_+ |\tilde{\mathcal{M}}_i||T_i|, \tag{97}$$

where the double integration is performed over the Dalitz plot surface.

We introduce also the modified annihilation (W-exchange) amplitudes A_i':

$$\tilde{\mathcal{M}}_i = T_i + A_i'. \tag{98}$$

As follows from Eqs. (65) and (91) these amplitudes are related to the tree and annihilation amplitudes:

$$A_i' = T_i(e^{-i\phi_4} - 1) + e^{-i\phi_4}A_i. \tag{99}$$

The formulas for the modified amplitudes A_i' can be rewritten in the same way as the corresponding formulas for the annihilation amplitudes if we introduce new coefficients replacing the former form factors calculated at the momentum transfer squared $m^2_{D^0}$. Thus, for example, the new coefficient $\tilde{A}_0^{\bar{K}^0 R_P[\pi^+\pi^-]}$ for the A_4' amplitude is given by the formula

$$\tilde{A}_0^{\bar{K}^0[\pi^+\pi^-]_P} = (e^{-i\phi_4} - 1)\frac{f_{K^0}}{f_{D^0}}A_0^{D^0 R_P[\pi^+\pi^-]}(m^2_{K^0}) + e^{-i\phi_4}A_0^{\bar{K}^0 R_P[\pi^+\pi^-]}(m^2_{D^0}). \tag{100}$$

Similar relations are valid for the new complex coefficients $\tilde{F}_0^{[\bar{K}^0\pi^-]_S\pi^+}$, $\tilde{F}_0^{\bar{K}^0[\pi^+\pi^-]_S}$, $\tilde{A}_0^{[\bar{K}^0\pi^-]_P\pi^+}$ and $\tilde{A}_0^{\bar{K}^0\omega}$, related to the amplitudes A_1', A_2', A_3', and A_5', respectively. By definition, the $\tilde{A}_0^{\bar{K}^0[\pi^+\pi^-]_P}$ coefficient is real. All the six new coefficients, defined above, will be extracted by fitting the Dalitz density distributions.

Due to our poor knowledge of the form factor combinations, defined in Eqs. (26) and (28) for the D waves, we are unable to calculate separately the tree contributions $\mathcal{T}_6$ and $\mathcal{T}_7$. Therefore in the following considerations leading to the possibly best determination of the lower limit of the annihilation branching fraction we have to omit temporarily from the total sum the contributions $\mathcal{M}_6$ and $\mathcal{M}_7$.

Denoting by $\mathcal{T}''$, $\mathcal{A}''$ and $\tilde{\mathcal{M}}''$ the sums of the tree, annihilation and modified partial amplitudes,

$$\mathcal{T}'' = \sum_{i\neq 6,7}\mathcal{T}_i, \quad \mathcal{A}'' = \sum_{i\neq 6,7}\mathcal{A}_i, \quad \tilde{\mathcal{M}}'' = \sum_{i\neq 6,7}\mathcal{M}_i, \tag{101}$$

and using Eq. (95) we obtain

$$\mathcal{A}'' = e^{i\phi_4}\tilde{\mathcal{M}}'' - \mathcal{T}''. \tag{102}$$

Then similar inequalities to those of Eq. (96) are satisfied:

$$|\tilde{\mathcal{M}}''|^2 + |\mathcal{T}''|^2 - 2|\tilde{\mathcal{M}}''||\mathcal{T}''| \le |\mathcal{A}''|^2 \le |\tilde{\mathcal{M}}''|^2 + |\mathcal{T}''|^2 + 2|\tilde{\mathcal{M}}''||\mathcal{T}''|, \tag{103}$$

from which we get the lower and upper limits of the total annihilation branching fractions

$$\mathrm{Br}''_{\mathrm{ann,low}} = \mathrm{Br}'' + \mathrm{Br}''_{\mathrm{tree}} - 2\iint ds\_ds_+|\tilde{\mathcal{M}}''||\mathcal{T}''| \tag{104}$$

and

$$\mathrm{Br}''_{\mathrm{ann,up}} = \mathrm{Br}'' + \mathrm{Br}''_{\mathrm{tree}} + 2\iint ds\_ds_+|\tilde{\mathcal{M}}''||\mathcal{T}''|. \tag{105}$$

Here Br'' is the total branching fraction for the decay process considered by us with exclusion of the amplitudes $\mathcal{T}_6$ and $\mathcal{T}_7$:

$$\mathrm{Br}'' = \iint ds\_ds_+|\tilde{\mathcal{M}}''|^2 \tag{106}$$

and $\mathrm{Br}''_{\mathrm{tree}}$ is defined as

$$\mathrm{Br}''_{\mathrm{tree}} = \iint ds\_ds_+|\mathcal{T}''|^2. \tag{107}$$

IV. INPUT DATA AND USEFUL FORMULAS

The calculation of the full amplitude derived in the preceding section requires the input of many physical ingredients in addition to a number of parameters which will be considered as free.

The Fermi coupling constant G_F is taken to be equal to 1.16637×10^{-5} GeV^{-2} [38]. The values of the CKM coupling matrix elements of Eq. (2) are, to order λ^4, where $\lambda = 0.2253$ is the sine of the Cabibbo angle [38] $\Lambda_1 \approx 1 - \lambda^2$ and $\Lambda_2 \approx -\lambda^2$. In the literature one can find many different values for the effective coefficients a_i, $i = 1, 2$. Reference [17] uses the leading order, $a_1 = 1.1463$, $a_2 = -0.2349$ while Ref. [16] approximates these by $a_1 = 1.15$, $a_2 = -0.25$. The phenomenological values $a_1 = 1.2 \pm 0.1$, $a_2 = -0.5 \pm 0.1$ have been introduced in Ref. [18]. Reference [21], invoking a large N_C approach, quotes the following $a_1 \simeq C_1(\bar{m}_c) = 1.274$ and $a_2 \simeq C_2(\bar{m}_c) = -0.529$ with $\bar{m}_c(m_c) = 1.25$ GeV, values extracted from Tables VI and VII of Ref. [32]. In Refs. [19], [21], and [22], the parameters a_1 and a_2 have been fitted to data for different kinds of two-body D-decays. Moreover, in Ref. [19] two additional phenomenological coefficients a_A and a_E have been included to account for the W-annihilation and W-exchange contributions. Let us note that in the factorization approach the coefficient a_E is equal to a_2 as follows from the derivation of our annihilation amplitudes in Sec. II.

All the annihilation amplitudes, proportional to a_2, can acquire strong phases related to the final state interactions described by the relevant form factors fixed at the momentum transfer squared $m^2_{D^0}$ [see Eqs. (42), (43), (46)–(48), (57), (62)]. Thus the a_2 phase cannot result from a fit to data. Furthermore, only the products of a_2 with the above-mentioned form factors can be well determined from the fit. Therefore in the present work we will adopt the real values

$$a_1 = 1.1 \qquad \text{and} \qquad a_2 = -0.5. \tag{108}$$

The amplitudes incorporate the π, K^0, ρ and D^0 meson decay constants as well as their masses and, when

appropriate, their widths. They are respectively, following mainly Ref. [38] except when otherwise stated:

$$f_\pi = 0.13041 \text{ GeV} \quad \text{and} \quad m_\pi = 0.13957 \text{ GeV}, \tag{109}$$

$$f_{K^-} = 0.1561 \text{ GeV} \quad \text{and} \quad m_{K^0} = 0.497614 \text{ GeV}, \tag{110}$$

$$f_\rho = 0.209 \text{ GeV} \tag{111}$$

$$m_\omega = 0.78265 \text{ GeV} \quad \text{and} \quad \Gamma_\omega = 0.00849 \text{ GeV}, \tag{112}$$

$$f_{D^0} = 0.2067 \text{ GeV}, \quad m_{D^0} = 1.86486 \text{ GeV} \quad \text{and} \quad \Gamma_{D^0} = 1.605 \times 10^{-12} \text{ GeV}. \tag{113}$$

The ρ decay constant is extracted from Ref. [13]. The D^0 decay constant is assimilated to the D^+ one, given in Ref. [38]. The mass and width of the $K^*(892)^\mp$ are considered as free parameters. Its decay constant, $f_{K^{*-}} = f_{K^{*+}} = 0.2143$ GeV, is taken from Ref. [25].

In addition, the mass and total width of the f_2 and K_2^* mesons read [38]

$$m_{f_2} = 1.2751 \text{ GeV} \quad \text{and} \quad \Gamma_{f_2} = 0.1851 \text{ GeV}, \tag{114}$$

$$m_{K_2^*} = 1.4256 \text{ GeV} \quad \text{and} \quad \Gamma_{K_2^*} = 0.0985 \text{ GeV}, \tag{115}$$

respectively.

We use $F_0^{D^0 R_S[\bar{K}^0\pi^-]}(m_\pi^2) = 0.48$ following Ref. [22] and $F_0^{D^0 R_S[\pi^+\pi^-]}(m_{K^0}^2) = 0.18$ according to Ref. [17]. We extract $A_0^{D^0 R_P[\bar{K}^0\pi^-]}(m_\pi^2) = 0.76$ from Table 9 of Ref. [39]. Although the values given in Table 14 of Ref. [15] are at zero momentum transfer, we assume here that $A_0^{D^0 R_P[\pi^+\pi^-]}(m_{K^0}^2) = 0.7$ and $A_0^{D^0\omega}(m_{K^0}^2) = 0.669$.

Finally, from Eq. (4.12) and Table 12 of Ref. [39], we have

$$F_0^{D^0\pi^-}(s_+) = \frac{F_0}{1 - \sigma_1 \frac{s_+}{M^2} + \sigma_2 \frac{s_+^2}{M^4}} \tag{116}$$

with $M = 2.01$ GeV, $\sigma_1 = 0.54$, $\sigma_2 = 0.32$ and $F_0 = 0.69$, and, from Eq. (4.10) and Table 12 of the same reference,

$$F_1^{D^0\pi^-}(s_+) = \frac{F_0}{(1 - \frac{s_+}{M^2})(1 - \sigma_1 \frac{s_+}{M^2})} \tag{117}$$

with $M = 2.01$ GeV, $\sigma_1 = 0.30$ and $F_0 = 0.69$.

The coupling constant $g_{\omega\pi\pi}$ is given by

$$g_{\omega\pi\pi} = m_\omega \sqrt{\frac{24\pi\Gamma_{\omega\pi\pi}}{p^3}} \quad \text{with} \quad p = \frac{1}{2}\sqrt{m_\omega^2 - 4m_\pi^2} \tag{118}$$

and, using $\Gamma_{\omega\pi\pi} = 0.0153$ $\Gamma_\omega = 1.299 \times 10^{-4}$ GeV, we have $g_{\omega\pi\pi} = 0.3504$.

The coupling constant $g_{f_2\pi^+\pi^-}$ in Eqs. (27) and (53) is defined as

$$g_{f_2\pi^+\pi^-} = m_{f_2} \sqrt{\frac{60\pi\Gamma_{f_2\pi^+\pi^-}}{q_{f_2}^5}}. \tag{119}$$

The partial width $\Gamma_{f_2\pi^+\pi^-}$ is given by

$$\Gamma_{f_2\pi^+\pi^-} = \frac{2}{3} 0.848 \Gamma_{f_2} \tag{120}$$

with Γ_{f_2} from Eq. (114), so that $\Gamma_{f_2\pi^+\pi^-} = 0.1046$ GeV and $g_{f_2\pi^+\pi^-} = 18.55$ GeV^{-1}.

The total width $\Gamma_{f_2}(s_0)$ reads [see, e.g. Eqs. (A.29) and (A.30) of Ref. [27]]

$$\Gamma_{f_2}(s_0) = \left(\frac{q}{q_{f_2}}\right)^5 \frac{m_{f_2}}{\sqrt{s_0}} \frac{(q_{f_2} r)^4 + 3(q_{f_2} r)^2 + 9}{(qr)^4 + 3(qr)^2 + 9} \Gamma_{f_2}, \tag{121}$$

with $r = 4.0$ GeV^{-1}.

The center-of-mass pion momenta that enter those expressions are respectively

$$q_{f_2} = \frac{1}{2}\sqrt{m_{f_2}^2 - 4m_\pi^2} \quad \text{and} \quad q = \frac{1}{2}\sqrt{s_0 - 4m_\pi^2}. \tag{122}$$

The coupling constant $g_{K_2^{*-}K_S^0\pi^-}$ appearing in Eqs. (24) and (52) is fixed at

$$g_{K_2^{*-}K_S^0\pi^-} = m_{K_2^{*-}} \sqrt{\frac{60\pi\Gamma_{K_2^{*-}K_S^0\pi^-}}{q_{K_2^*}^5}} = 11.72 \text{ GeV}^{-1} \tag{123}$$

with

$$q_{K_2^*} = \frac{1}{2m_{K_2^*}} \sqrt{[m_{K_2^*}^2 - (m_\pi + m_{K^0})^2][m_{K_2^*}^2 - (m_\pi - m_{K^0})^2]} \tag{124}$$

and

TABLE II. Values of the fixed form factors and coupling constants.

Parameter	Value
$F_0^{D^0 R_S[\bar{K}^0\pi^-]}(m_\pi^2)$	0.48
$F_0^{D^0 R_S[\pi^+\pi^-]}(m_{K^0}^2)$	0.18
$A_0^{D^0 R_P[\bar{K}^0\pi^-]}(m_\pi^2)$	0.76
$A_0^{D^0 R_P[\pi^+\pi^-]}(m_{K^0}^2)$	0.7
$A_0^{D^0\omega}(m_{K^0}^2)$	0.669
$g_{\omega\pi\pi}$	0.3504
$g_{f_2\pi^+\pi^-}$	18.55 GeV^{-1}
$g_{K_2^{*-}K^0\pi^-}$	11.72 GeV^{-1}

$$\Gamma_{K_2^{*-}K_S^0\pi^-} = \frac{2}{3} 0.489\ \Gamma_{K_2^*} = 0.0321\ \text{GeV}. \tag{125}$$

We take $g_{K_2^{*+}K_S^0\pi^+} = g_{K_2^{*-}K_S^0\pi^-}$.

To summarize this section, we have 33 free parameters: 14 complex parameters, namely, χ_1, χ_2, $\tilde{F}_0^{R_S[\bar{K}^0\pi^-]\pi^+}(m_{D^0}^2)$, $\tilde{F}_0^{\bar{K}^0 R_S[\pi^+\pi^-]}(m_{D^0}^2)$, $\tilde{A}_0^{R_P[\bar{K}^0\pi^-]\pi^+}(m_{D^0}^2)$, $\tilde{A}_0^{\bar{K}^0\omega}(m_{D^0}^2)$, q_6, s_6, q_7, s_7, q_{10}, s_{10}, z_8, z_9 and five real parameters, $\tilde{A}_0^{\bar{K}^0 R_P[\pi^+\pi^-]}(m_{D^0}^2)$, κ, c, $m_{K^{*\mp}}$, Γ_{K^*}. The parameters κ and c enter the pion scalar form factor [see Eqs. (28) and (39) in Ref. [27]]. The dominating P- and S-wave amplitudes require nine and 12 parameters, respectively, while the D amplitudes, whose magnitudes are much smaller, depend on 12 parameters.

In addition to a_1 and a_2 fixed at the values given in Eq. (108), and to the masses, widths and decay constants listed in Eqs. (109)–(115), Table II sums up the values of the fixed form factors and of the coupling constants needed in the calculations that follow.

V. RESULTS AND DISCUSSION

The free parameters of the $D^0 \to K_S^0\pi^+\pi^-$ decay amplitudes described in the preceding section are fitted to the 2010 the Belle collaboration data [10,30]. We have calculated the two-dimensional effective mass distribution corrected for background and efficiency variation as a function of Dalitz plot position. A grid of 125×125 squared cells covering the Dalitz plot in s_- and s_+ variables is constructed. For each cell a corresponding number of events is evaluated. The width of each cell is chosen to be $\Delta s = 0.02055\ \text{GeV}^2$. If the number of events in a given cell is smaller than 5 then the adjacent cells with the same s_- value are combined. If necessary, in the vicinity of the Dalitz plot edge, cells corresponding to s_- and $s_- + \Delta s$ values are grouped in order to accumulate more than five events. This allows a better application of mathematical methods to estimate the statistical errors ΔN^{exp} of the experimental event numbers N^{exp}. The total number of effective cells with N^{exp} greater than 5 is 6321. The total number of signal events in these cells is equal to 453876. The corresponding theoretical number of events N_j^{th} is calculated using the model density distribution integrated over the surface of a given cell j. The experimental finite effective mass resolution is taken into account by calculating the convolution of the theoretical distribution with the Gaussian function using its resolution parameter equal to $0.0055\ \text{GeV}^2$ [30]. The total number of events in the theoretical distribution is normalized to the experimental one. The parameter fitting procedure is based on the following definition of the χ_D^2 function:

$$\chi_D^2 = \sum_j \left[\frac{N_j^{\text{th}} - N_j^{\text{exp}}}{\Delta N_j^{\text{exp}}}\right]^2. \tag{126}$$

The statistical errors have been calculated as $\Delta N_j^{\text{exp}} = \sqrt{N_j^{\text{exp}}}$.

In the fitting procedure, as indicated in Sec. IV, the mass and width of the $K^*(892)$ meson are free parameters. These parameters enter also in the $K\pi$ vector form factor taken from the Belle collaboration fit to the $\tau^- \to K_S^0\pi^-\nu_\tau$ decays [28]. The contributions of $K^*(892)$ and $K^*(1410)$ resonances are taken into account but without that of the $K^*(1680)$ resonance. Including that resonance cannot improve the quality of the fit because its large mass is close to the upper limit of the $K\pi$ effective mass in the $D^0 \to K_S^0\pi^+\pi^-$ decay. The parameters of the $K^*(1410)$ resonance are fixed to the values given in the middle column of Table 3 in Ref. [28].

In order to have consistent $K^*(892)$ parameters we perform a simultaneous fit of the D^0 and τ decay data. The χ_τ^2 function is defined similarly to the χ_D^2 function of Eq. (126). We use the first 89 experimental points up to the $K\pi$ effective mass equal to 1.65 GeV covering a range where the statistical errors are not too large [28]. The $K\pi$ mass distribution is calculated with Eq. (2) of this reference. Alternatively to the experimental parametrization of Ref. [28] we use the model of the $K\pi$ vector form factor of Boito *et al.* [35] in which some constraints from analyticity and elastic unitarity are incorporated. We also found that the unitary $K\pi$ vector form factor derived and used in Ref. [25] to fit the $B \to K\pi^+\pi^-$ decay data gives $K^*(892)$ parameters in disagreement with those required here to fit well the present high statistics $D^0 \to K_S^0\pi^+\pi^-$ data. As mentioned in Sec. II A, the scalar $K\pi$ form factor is calculated as in Ref. [25]. Its functional form in the $K\pi$ effective mass range close to the position of the $K_0^*(1430)$ resonance depends sensitively on the f_K/f_π ratio of the kaon to pion coupling constants [40]. It is illustrated in Fig. 7. We find that the best fit is obtained with the $K\pi$ scalar form factor calculated with a f_K/f_π value of 1.175.

As pointed out below Eq. (16), two types of the pion vector form factor have been tested, namely the experimental parametrization used by the Belle collaboration in

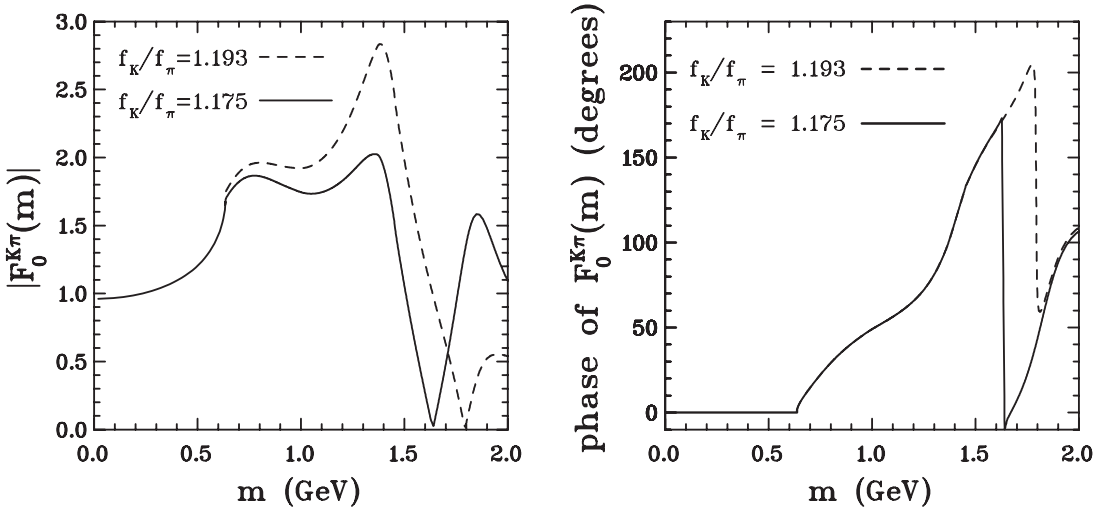

FIG. 7. The modulus (left panel) and the phase (right panel) of the $K\pi$ scalar form factor $F_0^{K\pi}$ as function of the $K\pi$ effective mass for two values of the f_K/f_π ratio.

the data analysis of the $\tau^- \to \pi^-\pi^0\nu_\tau$ decays [29] and the Hanhart model presented in Ref. [36].

We fit also the total experimental branching fraction of the $D^0 \to K^0_S\pi^+\pi^-$ decay, $\mathrm{Br}^{\mathrm{tot}}_{\mathrm{exp}} = (2.82 \pm 0.19)\%$ [38]. Denoting its contribution to the total χ^2 function as χ^2_{Br} we define

$$\chi^2 = \chi^2_D + \chi^2_\tau + w\chi^2_{\mathrm{Br}}, \tag{127}$$

where the weight w, in principle equals to 1, will be set so as to obtain reasonable value of the total branching fraction (see below). The total number of free parameters in our model being equal to 33, the number of degrees of freedom, ndf, in the fit is $\mathrm{ndf} = 6321 + 89 + 1 - 33 = 6378$. The combined D^0 and τ decay data fit leads, with $w = 1$, to $\chi^2 = 9451$ which gives $\chi^2/\mathrm{ndf} = 1.48$. The values of χ^2_D, χ^2_τ and χ^2_{Br} are equal to 9328, 123 and 0.04, respectively. The calculated total branching fraction is $\mathrm{Br}^{\mathrm{tot}} = 2.78\%$. This fit is obtained for the pion vector form factor calculated according to Hanhart's model with the 2 C fit parameters shown in Table 1 of Ref. [36]. For the $K\pi$ vector form factor we have used the Belle parametrization of Ref. [28]. The results quoted above have been obtained for the value of $f_K/f_\pi = 1.175$ which belongs to input parameters in the $K\pi$ scalar form factor as described in Ref. [25]. In studies of the B decays into $K\pi^+\pi^-$ [25] the value $f_K/f_\pi = 1.193$ has been used although it has already been noticed that the lower value of this ratio, 1.183, gave an improved χ^2. Here, for the $D^0 \to K^0_S\pi^+\pi^-$ decays, we have checked that with $f_K/f_\pi = 1.193$ one obtains a much worse fit with $\chi^2 = 10045$. However, if we lower the f_K/f_π value down to 1.165 the χ^2 rises again to 9979, being by 528 units higher than the minimum of $\chi^2 = 9451$ for $f_K/f_\pi = 1.175$. Thus the functional dependence of the scalar $K\pi$ form factor on the $K\pi$ effective mass plays a major role in finding the χ^2 minimum. Taking the vector $K\pi$ form factor of Boito *et al.* [35] instead of that from Belle parametrization [28] leads to slightly higher $\chi^2 = 9488$. The two sets of parameters obtained for $\chi^2 = 9451$ and for $\chi^2 = 9488$ will be discussed in more detail below. However, for the sake of completeness we quote the corresponding χ^2 values when the Hanhart's pion vector form factor is replaced by the Belle form factor of Ref. [29]. Then one gets still higher χ^2 values equal to 9514 and 9522, respectively.

The resulting values of parameters for the best fit are shown in Table III. As in the experimental analyses we fix the phase of the term multiplying the pion vector form factor $F_1^{\pi^+\pi^-}(s_0)$ to be zero. Consequently, the parameter $\tilde{A}_0^{\bar{K}^0 R_P[\pi^+\pi^-]}(m^2_{D^0})$ is real as explained in Sec. III B. This forces us to introduce a tilda on the other form factor parameters appearing in Table III to differentiate them from the physical form factors. The value of χ_1 can be estimated from a Breit-Wigner amplitude representation for the strange scalar meson $K^*_0(1430)$ whose decay into $K\pi$ dominates the $K\pi$ S wave. Using a formula similar to Eq. (18) of Ref. [23] with $|F_0^{\bar{K}^0\pi^-}(m^2_{K^*_0(1430)})| = 1.73$ [25] for $f_K/f_\pi = 1.175$ one obtains $\chi_1 = 5.6\ \mathrm{GeV}^{-1}$ which is close to the value $(5.43 \pm 0.22)\ \mathrm{GeV}^{-1}$ given in Table III. It is also comparable to the $\chi^{\mathrm{eff}}_S = (4.9 \pm 0.4)\ \mathrm{GeV}^{-1}$ obtained in the Dalitz plot analysis of the $D^+ \to K^-\pi^+\pi^+$ decay performed in Ref. [18], as can be seen from their Eq. (38). A similar estimation of χ_2 for the $[\pi^+\pi^-]$ S wave is unfeasible since in that channel one has three scalar resonances which cannot be properly approximated by Breit-Wigner functions so the χ_2 value represents an effective coupling. However, its value is compatible with the χ_{f_0} value of $(26 \pm 9)\ \mathrm{GeV}^{-1}$ obtained in Ref. [16] for the $D^+ \to \pi^+\pi^-\pi^+$ decays, as seen from their Eq. (46).

TABLE III. Parameters obtained from the best fit to the Belle data [10] ($\chi^2 = 9451$). The first error is statistical and the second one shows the modulus of the difference between the parameter value obtained in the fit using the $K\pi$ form factor of Boito *et al.* [35] ($\chi^2 = 9488$) and that of the best fit performed with the Belle parametrization [28] for this form factor.

Parameter	Modulus	Phase (deg)
χ_1	$5.43 \pm 0.22 \pm 0.00$	$248.1 \pm 1.3 \pm 2.0$
χ_2	$32.50 \pm 1.21 \pm 0.09$	$221.9 \pm 0.9 \pm 0.7$
$\tilde{F}_0^{\pi^+ R_S[\bar{K}^0\pi^-]}(m^2_{D^0})$	$1.94 \pm 0.03 \pm 0.00$	$245.6 \pm 1.1 \pm 1.1$
$\tilde{F}_0^{\bar{K}^0 R_S[\pi^-\pi^+]}(m^2_{D^0})$	$1.36 \pm 0.02 \pm 0.00$	$37.7 \pm 0.4 \pm 0.2$
$\tilde{A}_0^{\pi^+ R_P[\bar{K}^0\pi^-]}(m^2_{D^0})$	$0.95 \pm 0.05 \pm 0.06$	$294.2 \pm 2.2 \pm 11.9$
$\tilde{A}_0^{\bar{K}^0 R_P[\pi^-\pi^+]}(m^2_{D^0})$	$0.66 \pm 0.04 \pm 0.01$	0.0 (fixed)
$\tilde{A}_0^{\bar{K}^0\omega}(m^2_{D^0})$	$1.23 \pm 0.04 \pm 0.03$	$319.1 \pm 1.1 \pm 0.2$
q_6	$1.44 \pm 0.07 \pm 0.15$	$26.2 \pm 1.6 \pm 3.8$
s_6	$1.84 \pm 0.09 \pm 0.16$	$199.2 \pm 1.3 \pm 1.5$
q_7	$0.68 \pm 0.03 \pm 0.02$	$245.9 \pm 1.6 \pm 4.9$
s_7	$1.01 \pm 0.05 \pm 0.03$	$102.3 \pm 1.7 \pm 4.1$
z_8	$2.09 \pm 0.12 \pm 0.04$	$206.1 \pm 3.1 \pm 3.5$
z_9	$1.64 \pm 0.09 \pm 0.31$	$135.3 \pm 1.9 \pm 0.3$
q_{10}	$23.19 \pm 1.26 \pm 3.10$	$220.8 \pm 3.1 \pm 15.6$
s_{10}	$24.26 \pm 1.33 \pm 3.74$	$40.3 \pm 3.0 \pm 14.5$
c (GeV^{-4})	$0.29 \pm 0.02 \pm 0.02$	
κ (MeV)	$305.61 \pm 2.74 \pm 1.33$	
$m_{K^{*\mp}}$ (MeV)	894.74 ± 0.08	
Γ_{K^*} (MeV)	46.98 ± 0.18	

The parameters q_6, s_6, q_7, s_7, q_{10}, s_{10} are related to the D-wave contributions. As noted in Sec. III, the multiplicative complex parameters z_8 and z_9 entering the doubly Cabibbo suppressed $\mathcal{M}_8$ and $\mathcal{M}_9$ amplitudes can be interpreted in terms of some charge independence violation in the $[K\pi]_{S,P}\pi$ systems [see Eqs. (84) and (85)].

The parameters c and κ enter the calculation of the pion scalar form factor as described in chapter 3 of Ref. [27]. Figure 8 displays this form factor, obtained in the present fit to the Belle data compared to that calculated in the fit to the $B \to \pi\pi\pi$ data with $\kappa = 2$ GeV and $c = 19.5$ GeV^{-4} in Ref. [27]. In spite of the seemingly large differences observed, we have checked that, with the form factor fitted here to achieve the lowest χ^2_D for the $D^0 \to K^0_S\pi^+\pi^-$ decay, the main conclusions drawn in Ref. [27] for the $B \to \pi\pi\pi$ were not altered. This is due to the interplay between κ and c with the parameter χ_S in Ref. [27] and to the fact that the $B \to \pi\pi\pi$ data (see Ref. [41]) are statistically less restricting than the $D^0 \to K^0_S\pi^+\pi^-$ data. We also want to point out that the modulus of the pion scalar form factor is presently closer to that of the form factor calculated by Moussallam solving the Muskhelishvili-Omnès equations [42], notably below 1 GeV. Moussallam's form factor has been calculated for the meson-meson amplitudes taken from the three-channel model of Ref. [43] under an additional assumption that the off-diagonal matrix elements T_{13} and T_{23} are set equal to zero in the region below the third threshold ($m_0 < 1.4$ GeV). Moreover the cutoff energy E_0 defined in [42] has been chosen equal to 2 GeV.

The Dalitz plot density distribution that emerges from the fit of our model to the Belle data is plotted in Fig. 9. It displays a very rich interference pattern dominated by the presence of the $K^*(892)$ resonance. Figure 10 illustrates the distribution of χ^2 in the Dalitz plot. It shows that there is only a limited number of regions where the χ^2 exceeds 4 and, thus, that a good overall agreement of our model with the experimental density distribution of Ref. [10] is achieved. The mass and width of the charged $K^*(892)$ that come out of the minimization process are in very good agreement with the determination of the Belle collaboration for $\tau^- \to K^0_S\pi^-\nu_\tau$ decays [28].

In Ref. [2] the *BABAR* collaboration has reported results of their Dalitz plot analysis containing 540800 signal events for the $D^0 \to K^0_S\pi^+\pi^-$ decays. The Dalitz plot density distribution has been fitted using the isobar model with 43 free parameters. In the present paper, the values of the density distribution are calculated starting from a 1000×1000 grid tabulating the values of the *BABAR* model decay amplitude [31]. Summing these values in adjacent cells, one gets a set of pseudodata on a 125×125 grid with 7286 cells. Then the 33 free parameters of our model are fitted to these data using the same method as described above for the Belle data. The weight w of $\chi^2_{\rm Br}$ in Eq. (127) is increased by a factor 10 since with $w = 1$ one obtains a much too low value of Br$^{\rm tot}$ in comparison with the experimental value. Then, the total χ^2 equals to 6687 for ndf $= 7286 + 89 + 1 - 33 = 7343$ which gives $\chi^2/\text{ndf} = 0.91$. The values of χ^2_D, χ^2_τ and $\chi^2_{\rm Br}$ are 6533, 151 and 0.3, respectively (Br$^{\rm tot} = 2.71\%$). Taking as previously the alternative vector $K\pi$ form factor from Ref. [35] instead of that from Ref. [28] leads to a much higher $\chi^2 = 6951$.

Compared to Table III, Table IV reveals that the numerical values of the parameters fitted to the Belle data and to the *BABAR* model are quite close. Somehow indirectly this means that the Dalitz density distributions measured by both collaborations are very similar. Some noticeable differences between parameters are seen, mostly for the amplitudes whose contributions are small. In Fig. 11 two one-dimensional projections of the Dalitz density distributions are shown as an illustration of an overall agreement of the Belle data and the *BABAR* model.

The total branching fractions for different quasi-two-body channel amplitudes are given in Tables V and VI. The contribution of the $[K^0_S\pi^-]_P\pi^+$ amplitude is clearly dominant as was also found in the isobar model analysis for the $K^*(892)^-\pi^+$ of the Belle [1] and *BABAR* [2] collaborations. The four amplitudes $\mathcal{M}_1$, $\mathcal{M}_2$, $\mathcal{M}_3$ and $\mathcal{M}_4$ give

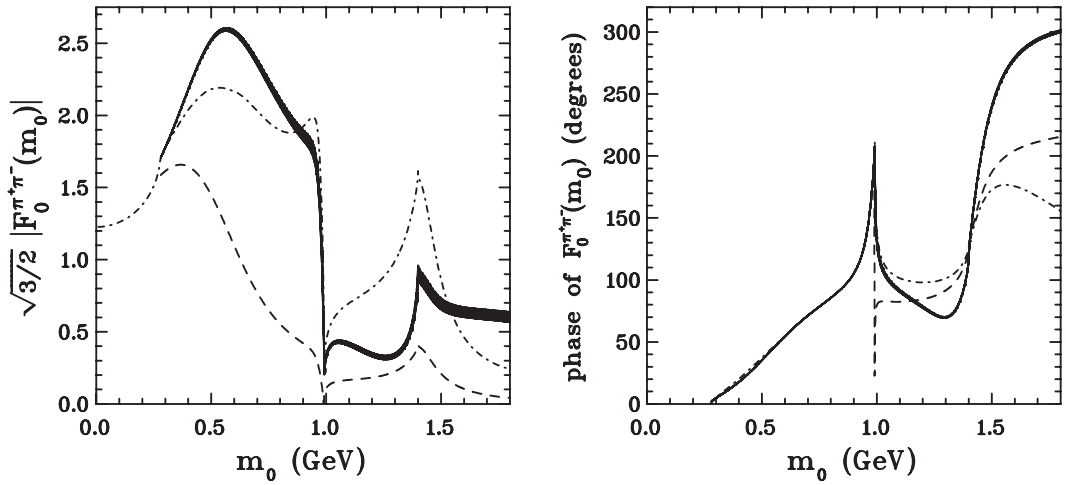

FIG. 8. The modulus (left panel) and the phase (right panel) of the pion scalar form factor $F_0^{\pi^+\pi^-}(m_0)$, obtained in the fit to the Belle data, is plotted as the dark band which represents its variation when the parameters κ and c vary within their errors given in Table III. It is compared with the same form factor introduced in Ref. [27] with the parameters $\kappa = 2$ GeV and $c = 19.5$ GeV^{-4} (dashed line) and with that calculated using the Muskhelishvili-Omnès equations [42] (dot-dashed line).

sizable contributions while the branching fractions of the remaining amplitudes are small. Our branching fraction for the $\mathcal{M}_3$ and $\mathcal{M}_4$ amplitudes compare well with the $K^*(892)\pi$ and $K_S^0\rho$ determinations of the experimental analyses [1,2,10].

The amplitudes $\mathcal{M}_1$ and $\mathcal{M}_2$, corresponding to the S-wave $K_S^0\pi$ and $\pi^+\pi^-$ subchannels, merge contributions from several resonances. Then, if one wishes, for example, to compare the branching fraction $(16.92 \pm 1.27)\%$ obtained for the amplitude $\mathcal{M}_2$ (see Table V) with the results of the Belle collaboration [10], one has to combine in the latter case the branching fractions for the following intermediate states: $K_S^0\sigma_1$, $K_S^0 f_0(980)$, $K_S^0\sigma_2$ and $K_S^0 f_0(1370)$. The sum of these four contributions, 18.16% compares well with the above value of our fit. Because of interferences between amplitudes the sum of the partial branching fractions differs from 100%. For example, for the fit to the Belle data it is equal to 132.8%, so that the total sum of the interference terms with respect to the total branching fraction amounts to −32.8%. The most important negative interference terms are equal to −26.4% for the amplitudes $\mathcal{M}_1$ and $\mathcal{M}_2$ and −10.1% for the amplitudes $\mathcal{M}_3$ and $\mathcal{M}_4$, respectively. There is also a positive interference term of 10.5% for the $\mathcal{M}_2$ and $\mathcal{M}_3$ amplitudes. Other interference contributions are much smaller.

As a consequence of the arbitrary choice of the $\mathcal{M}_4$ amplitude phase, one can only calculate the lower or upper limits of the branching fractions of the annihilation

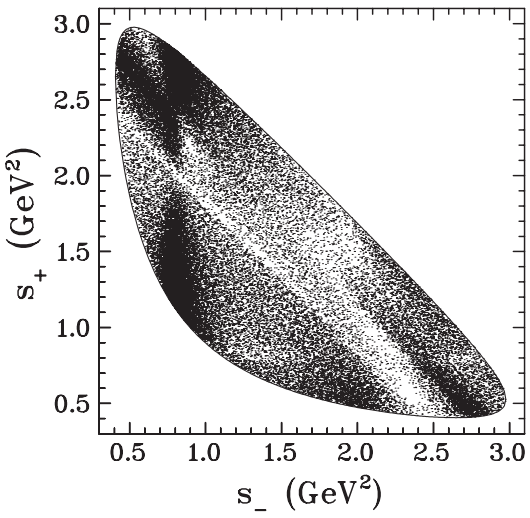

FIG. 9. Dalitz plot distribution from the fit to the Belle data [10].

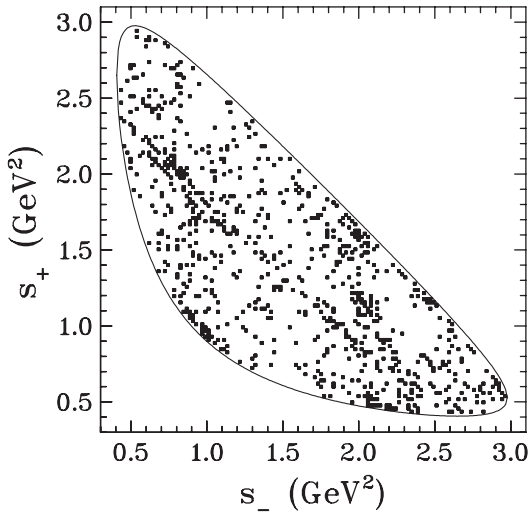

FIG. 10. Distribution of the χ^2 values inside the Dalitz plot contour drawn as a solid line. Black squares correspond to χ^2 values larger than 4.

TABLE IV. Parameters obtained from the best fit to the *BABAR* model data [31] ($\chi^2 = 6687$). The first error is statistical and the second one shows the modulus of the difference between the parameter value obtained in the fit using the $K\pi$ vector form factor of Boito *et al.* [35] ($\chi^2 = 6951$) and that of the best fit performed with the Belle parametrization [28] for this form factor.

Parameter	Modulus	Phase (deg)
χ_1	$5.08 \pm 0.10 \pm 0.03$	$229.0 \pm 1.1 \pm 2.0$
χ_2	$32.89 \pm 0.46 \pm 0.13$	$214.1 \pm 0.6 \pm 0.1$
$\tilde{F}_0^{\pi^+ R_S[\bar{K}^0\pi^-],}\ (m^2_{D^0})$	$1.99 \pm 0.03 \pm 0.00$	$262.8 \pm 1.0 \pm 1.2$
$\tilde{F}_0^{\bar{K}^0 R_S[\pi^-\pi^+]}\ (m^2_{D^0})$	$1.41 \pm 0.01 \pm 0.00$	$41.0 \pm 0.3 \pm 0.4$
$\tilde{A}_0^{\pi^+ R_P[\bar{K}^0\pi^-]}\ (m^2_{D^0})$	$0.96 \pm 0.02 \pm 0.05$	$287.5 \pm 0.9 \pm 10.8$
$\tilde{A}_0^{\bar{K}^0 R_P[\pi^-\pi^+]}\ (m^2_{D^0})$	$0.61 \pm 0.01 \pm 0.00$	0.0 (fixed)
$\tilde{A}_0^{\bar{K}^0\omega}\ (m^2_{D^0})$	$1.12 \pm 0.02 \pm 0.01$	$318.9 \pm 0.6 \pm 0.1$
q_6	$1.24 \pm 0.03 \pm 0.05$	$50.2 \pm 1.7 \pm 6.3$
s_6	$1.50 \pm 0.04 \pm 0.10$	$217.4 \pm 1.3 \pm 3.8$
q_7	$0.74 \pm 0.02 \pm 0.02$	$227.2 \pm 1.0 \pm 4.4$
s_7	$0.82 \pm 0.03 \pm 0.02$	$69.4 \pm 1.5 \pm 5.3$
z_8	$2.84 \pm 0.08 \pm 0.06$	$182.5 \pm 1.9 \pm 3.8$
z_9	$1.53 \pm 0.04 \pm 0.26$	$126.9 \pm 1.0 \pm 0.3$
q_{10}	$21.17 \pm 0.69 \pm 4.15$	$199.6 \pm 2.2 \pm 11.8$
s_{10}	$22.36 \pm 0.74 \pm 4.81$	$17.9 \pm 2.2 \pm 9.6$
c (GeV^{-4})	$0.19 \pm 0.01 \pm 0.02$	
κ (MeV)	$306.09 \pm 1.78 \pm 0.72$	
$m_{K^{*\mp}}$ (MeV)	894.31 ± 0.07	
Γ_{K^*} (MeV)	46.90 ± 0.15	

amplitudes (see derivation in Sec. III B). Their lower limits are displayed in Tables V and VI. These are sizable for the $\mathcal{M}_1$, $\mathcal{M}_2$, $\mathcal{M}_3$ and $\mathcal{M}_4$ cases. This points to the importance of the annihilation-diagram contributions. As can be seen from Eq. (96) in Sec. III B, the upper limits are larger than the sum of the branching fractions Br_i and $\mathrm{Br}_i^{\mathrm{tree}}$. Therefore they are not shown in Table V.

Lower limits, $\mathrm{Br}''_{\mathrm{ann.low}}$, of the summed annihilation amplitudes with the exclusion of the small components $\mathcal{M}_6$ and $\mathcal{M}_7$ can be calculated using Eq. (104). These divided by the fitted total branching fraction $\mathrm{Br}^{\mathrm{tot}}$ are $(20.0 \pm 2.5)\%$ and $(20.5 \pm 2.1)\%$, for the fits to the Belle data and to the *BABAR* model, respectively. The corresponding values of the tree branching fractions defined in Eq. (107) are 45.9% and 46.7% for the two cases considered here. Taking into account the above large values of the lower limits of the annihilation branching fractions, close to 20%, one must conclude that the annihilation contributions are important when compared with the tree amplitude terms.

The importance of the annihilation diagrams has also been pointed out in Refs. [19], [21], and [22]. In Ref. [19] a calculation of branching ratios for two-body hadronic decays of D and D_s mesons into pseudoscalar-pseudoscalar and pseudoscalar-vector mesons has been performed in a factorization approach for the "emission"-type diagrams and in a pole-dominance model for the annihilation-type diagrams. Relative strong phases between the different diagrams were introduced to obtain a better reproduction of the experimental data. As in our model, the contribution of the annihilation diagrams were found to be relatively large. An analysis of experimental data on branching fractions of charmed meson decays into pseudoscalar-pseudoscalar and

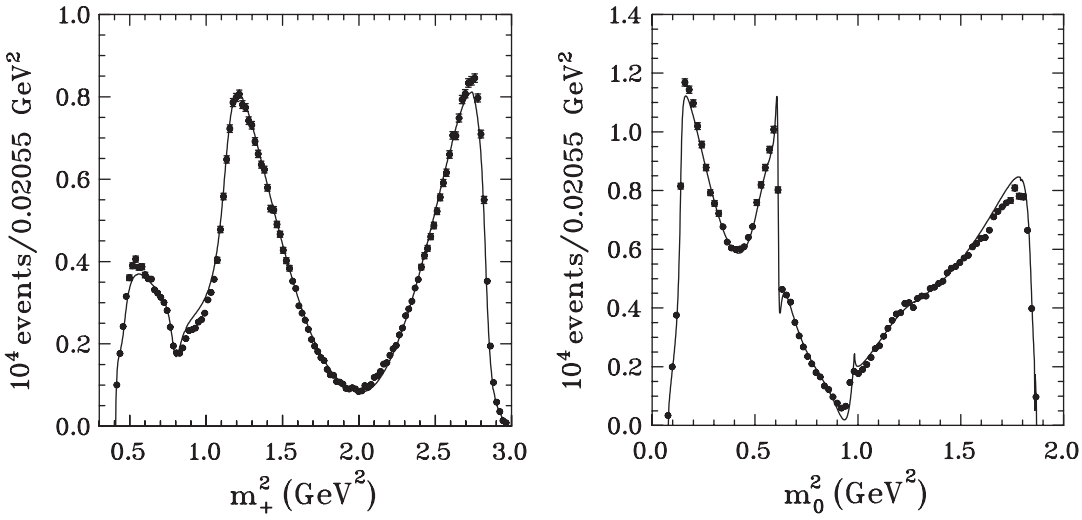

FIG. 11. Left panel: Comparison of the $K^0_S\pi^+$ effective mass squared distributions for the Belle data [10] (black dots) with the *BABAR* model [31] (solid curve), normalized to the number of events of the Belle experiment. Right panel: As in the left panel but for the $\pi^+\pi^-$ effective mass squared.

TABLE V. Branching fractions (Br) for different quasi-two-body channels calculated for the best fit to the Belle data [10] ($\chi^2 = 9451$). The sum of branching fractions is 132.81%. The branching fractions for the tree amplitudes (Tree), and the lower limits for the annihilation amplitudes (Ann. low) are also given. The first error of Br is statistical. The second error of Br and the errors of the tree and annihilation parts show the difference between the branching fractions obtained for the fit with $\chi^2 = 9488$ and those for the best fit (see Table III caption). All numbers are in percent.

Amplitude	Channel	Br	Tree	Ann. low
$\mathcal{M}_1$	$[K^0_S\pi^-]_S\pi^+$	$25.03 \pm 3.61 \pm 0.18$	8.24 ± 0.10	7.88 ± 0.11
$\mathcal{M}_2$	$K^0_S[\pi^-\pi^+]_S$	$16.92 \pm 1.27 \pm 0.02$	14.70 ± 0.17	2.92 ± 0.09
$\mathcal{M}_3$	$[K^0_S\pi^-]_P\pi^+$	$62.72 \pm 4.45 \pm 0.15$	24.69 ± 5.65	8.74 ± 2.97
$\mathcal{M}_4$	$K^0_S[\pi^-\pi^+]_P$	$21.96 \pm 1.55 \pm 0.06$	4.36 ± 0.06	6.74 ± 0.04
$\mathcal{M}_5$	$K^0_S\omega$	$0.79 \pm 0.07 \pm 0.04$	0.24 ± 0.01	0.16 ± 0.02
$\mathcal{M}_6$	$[K^0_S\pi^-]_D\pi^+$	$1.41 \pm 0.11 \pm 0.04$		
$\mathcal{M}_7$	$K^0_S[\pi^-\pi^+]_D$	$2.15 \pm 0.19 \pm 0.10$		
$\mathcal{M}_8$	$[K^0_S\pi^+]_S\pi^-$	$0.56 \pm 0.07 \pm 0.03$	0.07 ± 0.00	0.29 ± 0.02
$\mathcal{M}_9$	$[K^0_S\pi^+]_P\pi^-$	$0.64 \pm 0.06 \pm 0.02$	0.77 ± 0.15	0.01 ± 0.01
$\mathcal{M}_{10}$	$[K^0_S\pi^+]_D\pi^-$	$0.63 \pm 0.07 \pm 0.11$	0	0.63 ± 0.11

pseudoscalar-vector mesons has been performed in Ref. [21] using a quark-diagram approach. It suggests that W-exchange topology must play an important role. A comparison with the factorization procedure allowed to extract information on the effective Wilson coefficients and to discriminate between different solutions obtained in the diagrammatic scheme. The flavor-diagram approach has also been used in Ref. [22] to study D and D_s decays into a pseudoscalar meson and an even-parity scalar or axial vector or tensor meson. It was found that the contribution of annihilation diagrams could be important. The factorization formalism has also been used as a complementary tool to calculate some decay rates and again the inclusion of weak annihilation processes was found to be necessary to account for the data.

Dalitz plot projections or one-dimensional effective mass distributions are obtained by proper integration of the Dalitz plot density distributions. They are shown in Figs. 12, 13, and 14. The experimental $K^0_S\pi^-$ mass distribution in Fig. 12, dominated by the $K^*(892)$ resonance, is well reproduced by our model. In the right panel of this figure, where the vertical scale is expanded, some discrepancies above 2 GeV^2 are apparent. A good agreement between the model and data is seen in the left panel Fig. 13 showing the $K^0_S\pi^-$ distributions. The two prominent peaks, together with the minimum separating them, arise from the $K^*(892)^-$ resonance contribution. The left maximum is mainly associated with the $\rho(770)^0$ while the minimum, in the vicinity of 0.8 GeV^2, comes from interferences with the $K^*(892)^+$ resonance. The maxima at 1.2 and at 2.75 GeV^2, and the deep minimum at about 2 GeV^2 are due to a typical P-wave dependence of the $\mathcal{M}_3$ amplitude dominated by the $K^*(892)^-$ resonance.

TABLE VI. Branching fractions (Br) for different quasi-two-body channels calculated for the best fit to the *BABAR* model data [2] ($\chi^2 = 6687$). The sum of branching fractions is 138.77%. The branching fractions for the tree amplitudes (Tree), and the lower limits for the annihilation amplitudes (Ann. low) are also given. The first error of Br is statistical. The second error of Br and the errors of the tree and annihilation parts show the difference between the branching fractions obtained for the fit with $\chi^2 = 6951$ and those for the best fit (see Table IV caption). All numbers are in percent.

Amplitude	Channel	Br	Tree	Ann. low
$\mathcal{M}_1$	$[K^0_S\pi^-]_S\pi^+$	$30.11 \pm 1.25 \pm 0.03$	7.40 ± 0.13	10.64 ± 0.04
$\mathcal{M}_2$	$K^0_S[\pi^-\pi^+]_S$	$21.57 \pm 0.55 \pm 0.25$	16.25 ± 0.12	4.20 ± 0.16
$\mathcal{M}_3$	$[K^0_S\pi^-]_P\pi^+$	$60.36 \pm 1.39 \pm 0.28$	25.33 ± 5.60	7.53 ± 2.77
$\mathcal{M}_4$	$K^0_S[\pi^-\pi^+]_P$	$20.79 \pm 0.21 \pm 0.11$	4.48 ± 0.03	5.96 ± 0.03
$\mathcal{M}_5$	$K^0_S\omega$	$0.64 \pm 0.02 \pm 0.01$	0.25 ± 0.00	0.09 ± 0.00
$\mathcal{M}_6$	$[K^0_S\pi^-]_D\pi^+$	$1.38 \pm 0.04 \pm 0.06$		
$\mathcal{M}_7$	$K^0_S[\pi^-\pi^+]_D$	$1.75 \pm 0.07 \pm 0.12$		
$\mathcal{M}_8$	$[K^0_S\pi^+]_S\pi^-$	$0.99 \pm 0.06 \pm 0.06$	0.13 ± 0.00	0.50 ± 0.03
$\mathcal{M}_9$	$[K^0_S\pi^+]_P\pi^-$	$0.64 \pm 0.03 \pm 0.02$	0.68 ± 0.11	0.00 ± 0.00
$\mathcal{M}_{10}$	$[K^0_S\pi^+]_D\pi^-$	$0.54 \pm 0.03 \pm 0.15$	0	0.54 ± 0.15

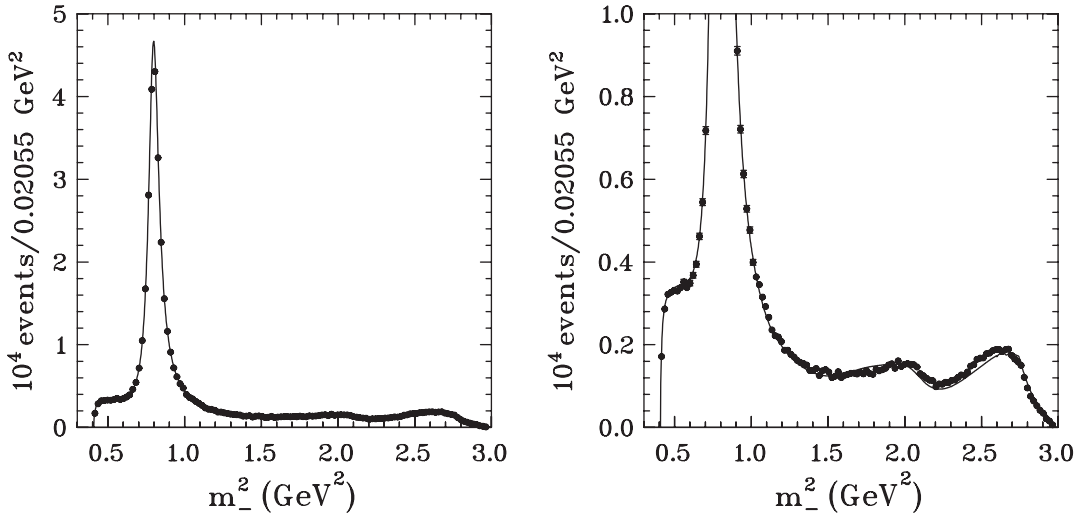

FIG. 12. Comparison of the $K^0_S\pi^-$ effective mass squared distributions for our model (solid curve) with the Belle data [10] (points with error bars). In the right panel the vertical scale is enlarged by a factor of 5 in order to enforce the differences at higher $K^0_S\pi^-$ masses.

The right panel of Fig. 13 shows the very rich structure of the Belle data which is well reproduced by our model. It exhibits clearly the $\pi^+\pi^-$ S-, P- and D-wave resonance effects. The first peak comes mainly from the $K^*(892)^+$ and $f_0(500)$, the second one from the $\rho(770)^0$, the strong decrease on its right being due to its interference with the narrow $\omega(782)$, the $f_0(980)$ being responsible for the deep minimum near 1 GeV^2, the $f_2(1270)$ contributes to the rise around 1.5 GeV^2, the right-hand side bump being dominated once more by the $K^*(892)^+$.

In Fig. 14 our m^2_+ and m^2_0 distributions are compared with the distributions calculated for the *BABAR* model. A noticeable deviation is seen for values of m^2_0 around 1.2 GeV^2 where the *BABAR* model shows a shoulder. The corresponding shoulder is also observed in the right panel of Fig. 13 for the Belle data. To account for the presence of such a structure near 1.2 GeV^2, a scalar resonance term called σ_1, with a mass of (1033 ± 7) MeV and a width of (88 ± 7) MeV, has been introduced in Ref. [10]. In Ref. [2] the K-matrix parametrization of the $\pi\pi$ S-wave state with a coupling to the $\eta\eta$ channel is introduced. The threshold mass squared corresponding to opening of the $\eta\eta$ channel is indeed equal to 1.201 GeV^2 and coincides with localization of the structure seen in Fig. 14 (dashed line). However, as seen in Fig. 3 of Ref. [2] this structure is rather wide. So, on the basis of experimental data for the m^2_0 distributions it is difficult to identify clearly the origin of this rather wide structure seen by both collaborations at 1.2 GeV^2. In our pion scalar form factor shown in Fig. 8, one does not observe a sharp structure near 1.1 GeV. Further studies of

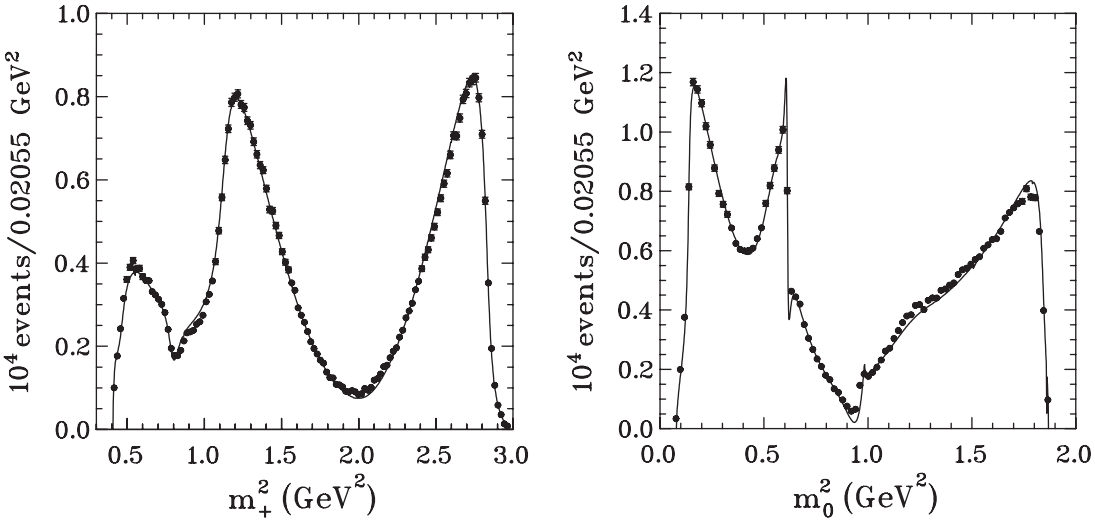

FIG. 13. Left panel: Comparison of the $K^0_S\pi^+$ effective mass squared distributions for the best fit (solid curve) with the Belle data [10] (points with error bars). Right panel: As in the left panel but for the $\pi^+\pi^-$ effective mass squared.

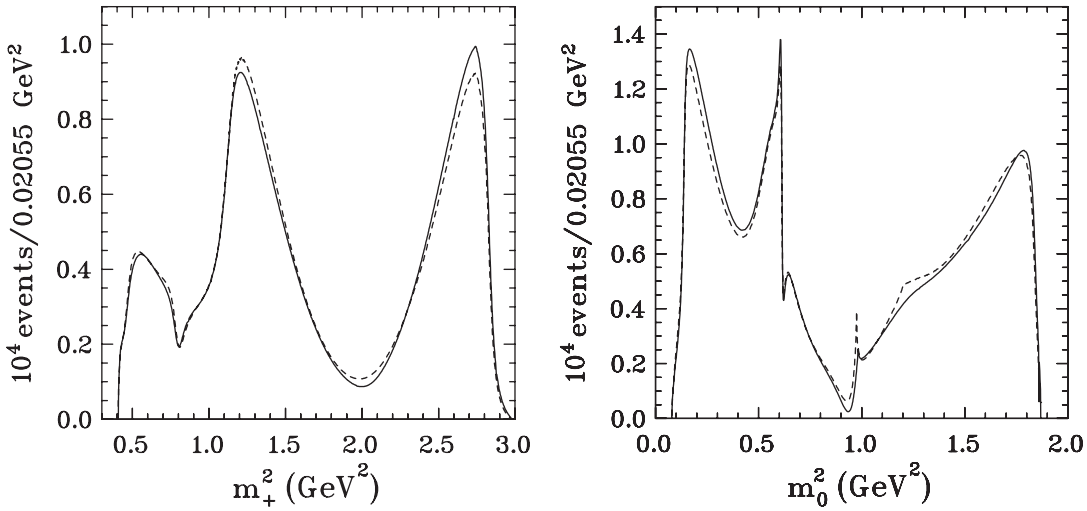

FIG. 14. Left panel: Comparison of the $K_S^0\pi^+$ effective mass squared distributions for the best fit (solid curve) with the *BABAR* model [31] (dashed curve). Right panel: As in the left panel but for the $\pi^+\pi^-$ effective mass squared.

different coupled channel production processes are needed to resolve this structure question.

VI. SUMMARY

We have used the quasi-two-body factorization to analyze the high-statistics data of the $D_S^0 \to K_S^0\pi^+\pi^-$ decay process measured by the Belle [1] and *BABAR* [2] collaborations. The three-meson final states are assumed to be the combinations of a meson pair in S-, P- and D waves and an isolated meson, leading to the quasi-two-body channels, $[K_S^0\pi^+]_{S,P,D}\pi^-$, $[K_S^0\pi^-]_{S,P,D}\pi^+$ and $K_S^0[\pi^+\pi^-]_{S,P,D}$. The decay amplitudes, built from the weak effective Hamiltonian, consist of Cabibbo favored (proportional to $V_{cs}^*V_{ud}$) and doubly Cabibbo suppressed (proportional to $V_{cd}^*V_{us}$) tree and W-exchange parts. All amplitudes are given in terms of superpositions of the effective Wilson coefficients and of the product of two transition matrix elements. The CF tree amplitudes are proportional to the product of the pion or kaon decay constant by the transition matrix element between the D^0 and $[K\pi]_{S,P,D}$ or $[\pi^+\pi^-]_{S,P,D}$ states, respectively. One DCS tree amplitude is proportional to the scalar or vector $K\pi$ form factor multiplied by the D^0 transition to the pion. The other DCS tree amplitude is proportional to the kaon decay constant times the D^0 transition to the $[\pi\pi]_{S,P,D}$ states. The W-exchange (or annihilation) amplitudes are proportional to the product of the D^0 decay constant by the form factor of the meson pair transition to a pion or a kaon.

We calculate the different transition matrix elements assuming that the meson pair involved goes first through the dominant intermediate resonance of this pair. The $K_0^*(1430)$, $K^*(892)$ and $K_2^*(1430)$ are the dominant resonances for the S, P, and D waves of the $[K\pi]_{S,P,D}$ states, respectively and the $f_0(980)$, $\rho(770)^0$, and $f_2(1270)$ for those of the $[\pi\pi]_{S,P,D}$ states. We then introduce the relevant vertex function to describe the decays of the resonant meson-pair state into the final meson pair. We further express this vertex function as being proportional to the kaon-pion or pion-pion scalar, vector or tensor form factors. We use the unitary $K\pi$ and $\pi\pi$ scalar form factors calculated with analyticity and chiral symmetry constraints in Refs. [25] and [27], respectively. These functions describe the $K_0^*(800)$, $K_0^*(1430)$ and the $f_0(500)$, $f_0(980)$ and $f_0(1400)$ scalar resonances contributions to the $K\pi$ and $\pi\pi$ final state interactions. The Belle analysis of the $\tau^- \to K_S^0\pi^-\nu_\tau$ [28] and Hanhart's model [36] of the $\tau^- \to \pi^-\pi^0\nu_\tau$ [29] decays yield the vector form factors. The $D^0 \to \omega(782)[\to \pi^+\pi^-]K_S^0$ decay amplitude is also added. The tensor vertex functions are parametrized by relativistic Breit-Wigner formulas.

Our 27 nonzero amplitudes are then combined into ten effective independent amplitudes. The reduction in the number of effective amplitudes, as compared to the isobar analyses, results from the factorization hypothesis. This leads to parametrization in terms of transition matrix elements which can be form factors or chosen to be proportional to form factors in which resonances are grouped together.

A χ^2 fit to a Dalitz plot data sample of the Belle collaboration analysis [30] is performed to determine the 33 free parameters of our $D^0 \to K_S^0\pi^+\pi^-$ decay amplitude. Our parameters are mainly related to the strength of the $[K\pi]_S$ and $[\pi\pi]_S$ scalar form factors and to the unknown meson to meson transition form factors at a large momentum transfer squared equal to $m_{D^0}^2$.

The fit to the data is very sensitive to the values of the mass and width of the $K^*(892)$ resonance. We include them in the fit, performing a combined analysis of the $D^0 \to K_S^0\pi^+\pi^-$ and $\tau^- \to K_S^0\pi^-\nu_\tau$ decay data. The total

experimental branching fraction is also fitted. An overall good fit, with a $\chi^2/\mathrm{ndf} = 1.48$ for a number of degree of freedom, $\mathrm{ndf} = 6378$, is carried out. Another set of amplitudes fits the *BABAR* collaboration Dalitz plot model of Ref. [31] with a $\chi^2/\mathrm{ndf} = 0.91$ for $\mathrm{ndf} = 7343$. The parameters of both fits are close, which indicates similar Dalitz density distribution measurements for both collaborations.

The Dalitz plot distribution of our fit to the Belle data [10] exhibits a very rich interference pattern governed by the $K^*(892)^-$ resonance. A good overall agreement with the experimental density distribution of Ref. [10] has been achieved. The corresponding one-dimensional effective mass distributions compare well those of Belle [10] or *BABAR* [31] and show the contributions of the different $K\pi$ [$K_0^*(800)$, $K^*(892)$, $K_0^*(1430)$] and $\pi\pi$ [$f_0(500)$, $f_0(980)$, $\rho(770)^0$, $\omega(782)$, $f_2(1270)$] resonances and of their interferences. The small bulge in the slope of the $\pi^+\pi^-$ effective mass squared distribution seen in the Belle and *BABAR* data at 1.2 GeV^2 might be associated with the coupling of the $\pi\pi$ channel to the $\eta\eta$ one. Our model, which does not include this coupling, does not exhibit such a behavior. Investigations on this matter would be worthwhile.

The branching fraction calculations show the dominance of the quasi-two-body channel $[K_S^0\pi^-]_P\pi^+$ with a branching fraction $\mathrm{Br} = (62.7 \pm 4.5)\%$ close to the values found in the isobar Belle [1] or *BABAR* [2] models for the $K^*(892)^-\pi^+$ amplitude. The next important contributions come from the $[K_S^0\pi^-]_S\pi^+$ amplitude with a Br of $(25.60 \pm 3.6)\%$, from the $K_S^0[\pi^-\pi^+]_P$ one, with a Br of $(22.0 \pm 1.6)\%$ and from the $K_S^0[\pi^-\pi^+]_S$ one with a Br of $(16.9 \pm 1.3)\%$. Branching fractions for the other amplitudes, $K_S^0[\pi^-\pi^+]_\omega$, $[K_S^0\pi^-]_D\pi^+$, $K_S^0[\pi^-\pi^+]_D$, $[K_S^0\pi^+]_S\pi^-$, $[K_S^0\pi^+]_P\pi^-$ and $[K_S^0\pi^+]_D\pi^-$ are small. The importance of the interference contributions (-32.8%) is seen in the fact that the total sum of all the branching fractions is larger than 100%.

The branching fractions corresponding to the quasi-two-body channel tree amplitudes give sizable contributions. The knowledge of the branching fractions does not allow to calculate all phases of our amplitudes, as it is the modulus square of the amplitudes which appears in the branching fraction formula. One of the phases of our ten amplitudes cannot be determined. We proceed as in the isobar model analysis in requiring the phase of the term multiplying the pion vector form factor in the $K_S^0[\pi^-\pi^+]_P$ amplitude to be zero. Consequently, we can predict only lower or upper limits of the branching fraction contributions of the annihilation amplitudes. We find that these lower limits can be sizable for the important quasi-two-body channels, $[K_S^0\pi^-]_P\pi^+$, $[K_S^0\pi^-]_S\pi^+$, $K_S^0[\pi^-\pi^+]_P$ and $K_S^0[\pi^-\pi^+]_S$ and we can say that, compared to the tree amplitudes, the annihilation ones have a significant contribution. The analyses of the two-body hadronic decays of D and D_s mesons in Refs. [19], [21], and [22] have also pointed out the importance of the annihilation diagrams.

As we do not know the $\bar{K}_0$ to $\rho(770)^0$ transition form factor value at the D^0 mass squared, our fit cannot be used to estimate the physical unknown π or K meson to $K\pi$ or $\pi\pi$ meson pair transition form factors entering the annihilation amplitudes. The full knowledge of the strong interaction meson-meson form factors can be obtained only if the strong meson-meson interaction is known at all energies [44]. Consequently, some information on the $\bar{K}_0\rho(770)^0$ strong interaction would be required to estimate the $\bar{K}_0$ to $\rho(770)^0$ transition form factor. It would be of interest if the unknown form factors entering the present model could be evaluated.

VII. CONCLUDING REMARKS AND PERSPECTIVES

In our quasi-two-body factorization approach the *CP* asymmetry, proportional to the very small imaginary part of $V_{cd}^*V_{us}$, is found to be of the order of 10^{-4}. This is in agreement with present observations [3,4] and values predicted by the standard model in the charm sector. Our $D^0 \to K_S^0\pi^+\pi^-$ decay amplitudes could be useful input for calculations of D^0-$\bar{D}^0$ mixing [1,2] and determination ([5–10]) of the CKM angle γ (or ϕ_3). Upon request we can provide numerical values of our amplitudes. The kaon-pion and pion-pion scalar form factors, entering our quasi-two-body factorization decay amplitude and built using other experimental data, are constrained by the present Dalitz plot analysis of the weak process $D^0 \to K_S^0\pi^+\pi^-$. In principle our analysis could also give constraints on πK and $\pi\pi$ tensor resonances. There have been recent observations (see e.g. Refs. [45,46]) of D and D_s excited states which can be formed due to the πD and KD strong interactions, respectively. Their properties could be used to constrain theoretical πD and KD scattering models and possibly also πD and KD transition form factors.

Taking advantage of the coupling between the $\pi\pi$ and the KK channels and extending the derivation of the unitary pion form factor [27] to that of the kaon, two of the present authors, Leśniak and Kamiński, together with two collaborators, have recently studied, in the quasi-two-body QCD factorization approach, the $B^\pm \to K^+K^-K^\pm$ decays [47]. We could also extend our present work to study, in the quasi-two-body factorization framework, the $D^0 \to K_S^0K^+K^-$ data analyzed by the *BABAR* [2], CLEO [5], and, more recently, by the LHCb [6] collaborations. A good knowledge of the $D^0 \to K_S^0K^+K^-$ decay amplitudes will also help in the determinations of the D^0-$\bar{D}^0$ mixing [2] and of the CKM angle γ [5,6].

ACKNOWLEDGMENTS

We are deeply indebted to Anton Poluektov from the Belle collaboration and Fernando Martinez-Vidal from the *BABAR* collaboration who provided vital information for

this study. We thank them for many fruitful exchanges. Anze Zupanc must be thanked for useful exchanges about the Belle data. We appreciate the help of Bachir Moussallam who supplied various numerical tables for the $K\pi$ scalar form factors used in this work. We would like to thank Christoph Hanhart for sending us tables of the pion vector form factor. The authors are obliged to Diogo Boito for useful correspondence and sending numerical values of his $K\pi$ vector form factor. We also thank Agnieszka Furman for her contribution in an early stage of this work. Fruitful discussions with Pascal David are gratefully recognized. This work has been partially supported by a grant from the French-Polish exchange program COPIN/CNRS-IN2P3, collaboration 08-127.

APPENDIX: ON KINEMATICS

In this Appendix, we recall some kinematic formulas useful for the calculation of our amplitudes. These kinematic expressions can also be found in Appendix A of Ref. [48]. For the $[K^0_S\pi^-]_L\pi^+$ amplitudes, in the $[K^0_S\pi^-]$ center-of-mass system defined by $\mathbf{p}_0+\mathbf{p}_-=0$, using Eqs. (3) and (4), one finds

$$\mathbf{p_1}=\mathbf{p_0}=-\mathbf{p}_- \quad \text{and}$$
$$|\mathbf{p}_1|=\frac{\sqrt{[s_- -(m_{K^0}+m_\pi)^2][s_- -(m_{K^0}-m_\pi)^2]}}{2m_-} \tag{A1}$$

and

$$|\mathbf{p}_+|=\frac{\sqrt{[m^2_{D^0}-(m_-+m_\pi)^2][m^2_{D^0}-(m_--m_\pi)^2]}}{2m_-}. \tag{A2}$$

From Eq. (3) one obtains

$$4\mathbf{p}_1\cdot\mathbf{p}_+=s_0-s_+ +\frac{(m^2_{D^0}-m^2_\pi)(m^2_{K^0}-m^2_\pi)}{s_-}, \tag{A3}$$

a factor which enters the $[\bar{K}^0\pi^-]_P\pi^+$ amplitude, Eq. (15).

In the $[\pi^+\pi^-]$ center-of-mass system, defined by $\mathbf{p}_+ + \mathbf{p}_- = 0$, one has

$$\mathbf{p_2}=\mathbf{p}_+=-\mathbf{p}_- \quad \text{and} \quad |\mathbf{p_2}|=\frac{1}{2}\sqrt{s_0-4m^2_\pi} \tag{A4}$$

and

$$|\mathbf{p}_0|=\frac{\sqrt{[m^2_{D^0}-(m_0+m_{K^0})^2][m^2_{D^0}-(m_0-m_{K^0})^2]}}{2m_0}. \tag{A5}$$

The scalar product $\mathbf{p}_2\cdot\mathbf{p}_0$, given by

$$4\mathbf{p}_2\cdot\mathbf{p}_0=s_- -s_+, \tag{A6}$$

enters the $\bar{K}^0[\pi^+\pi^-]_P$ amplitude, Eq. (16).

The analogous formulas for the $[K^0_S\pi^+]_L\pi^-$ amplitudes, in the $[K^0_S\pi^+]$ center-of-mass system, are obtained by exchanging subscripts $-$ and $+$ in Eqs. (A1), (A2), and (A3). Then p_1 becomes p_3 and p_+ is changed into p_- [see e.g. the corresponding $[K^0\pi^+]_P\pi^-$ amplitude, Eq. (31)].

[1] L. M. Zhang *et al.* (Belle Collaboration), Phys. Rev. Lett. **99**, 131803 (2007).
[2] P. del Amo Sanchez *et al.* (BABAR Collaboration), Phys. Rev. Lett. **105**, 081803 (2010); arXiv:1004.5053v3.
[3] D. M. Asner *et al.* (CLEO Collaboration), Phys. Rev. D **70**, 091101(R) (2004).
[4] T. Aaltonen *et al.* (CDF Collaboration), Phys. Rev. D **86**, 032007 (2012).
[5] J. Libby *et al.* (CLEO Collaboration), Phys. Rev. D **82**, 112006 (2010).
[6] R. Aaij *et al.* (LHCb Collaboration), Phys. Lett. B **718**, 43 (2012).
[7] H. Aihara *et al.* (Belle Collaboration) Phys. Rev. D **85**, 112014 (2012).
[8] P. del Amo Sanchez *et al.* (BABAR Collaboration), Phys. Rev. Lett. **105**, 121801 (2010).
[9] J. P. Lees *et al.* (BABAR Collaboration), Phys. Rev. D **87**, 052015 (2013).
[10] A. Poluektov *et al.* (Belle Collaboration), Phys. Rev. D **81**, 112002 (2010).
[11] H. Kamano, S. X. Nakamura, T.-S. H. Lee, and T. Sato, Phys. Rev. D **84**, 114019 (2011).
[12] P. C. Magalhães, M. R. Robilotta, K. S. F. F. Guimarães, T. Frederico, W. de Paula, I. Bediaga, A. C. dos Reis, C. M. Maekawa, and G. R. S. Zarnauskas, Phys. Rev. D **84**, 094001 (2011).
[13] M. Beneke and M. Neubert, Nucl. Phys. **B675**, 333 (2003).
[14] M. Wirbel, B. Stech, and M. Bauer, Z. Phys. C **29**, 637 (1985).
[15] M. Bauer, B. Stech, and M. Wirbel, Z. Phys. C **34**, 103 (1987).

[16] D. R. Boito, J.-P. Dedonder, B. El-Bennich, O. Leitner, and B. Loiseau, Phys. Rev. D **79**, 034020 (2009).
[17] B. El-Bennich, O. Leitner, J.-P. Dedonder, and B. Loiseau, Phys. Rev. D **79**, 076004 (2009).
[18] D. R. Boito and R. Escribano, Phys. Rev. D **80**, 054007 (2009).
[19] F.-S. Yu, X.-X. Wang, and C.-D. Lu, Phys. Rev. D **84**, 074019 (2011).
[20] A. J. Buras, Nucl. Phys. **B434**, 606 (1995).
[21] H.-Y. Cheng and C.-W. Chiang, Phys. Rev. D **81**, 074021 (2010).
[22] H.-Y. Cheng and C.-W. Chiang, Phys. Rev. D **81**, 074031 (2010).
[23] A. Furman, R. Kamiński, L. Leśniak, and B. Loiseau, Phys. Lett. B **622**, 207 (2005).
[24] B. El-Bennich, A. Furman, R. Kamiński, L. Leśniak, and B. Loiseau, Phys. Rev. D **74**, 114009 (2006).
[25] B. El-Bennich, A. Furman, R. Kamiński, L. Leśniak, B. Loiseau, and B. Moussallam, Phys. Rev. D **79**, 094005 (2009).
[26] O. Leitner, J.-P. Dedonder, B. Loiseau, and R. Kamiński, Phys. Rev. D **81**, 094033 (2010).
[27] J.-P. Dedonder, A. Furman, R Kamiński, L. Leśniak, and B. Loiseau, Acta Phys. Pol. B **42**, 2013 (2011).
[28] D. Epifanov *et al.* (Belle Collaboration), Phys. Lett. B **654**, 65 (2007). We use the data corrected for acceptance from http://www.slac.stanford.edu/xorg/hfag/tau/summer-2011/.
[29] M. Fujikawa *et al.* (Belle Collaboration), Phys. Rev. D **78**, 072006 (2008).
[30] A. Poluektov has provided us with a Dalitz plot data sample of the 2010 Belle collaboration analysis [10] (private communication).
[31] F. Martinez-Vidal (private communication). The BABAR model is based on a fit to the Dalitz-plot data of Ref. [2].
[32] G. Buchalla, A. J. Buras, and M. E. Lautenbacher, Rev. Mod. Phys. **68**, 1125 (1996).
[33] A. Ali, G. Kramer, and C.-D. Lü, Phys. Rev. D **58**, 094009 (1998).
[34] B. Moussallam, Eur. Phys. J. C **53**, 401 (2008).
[35] D. R. Boito, R. Escribano, and M. Jamin, J. High Energy Phys. 09 (2010) 031.
[36] C. Hanhart, Phys. Lett. B **715**, 170 (2012).
[37] C. S. Kim, J.-P. Lee, and S. Oh, Phys. Rev. D **67**, 014002 (2003).
[38] J. Beringer *et al.* (Particle Data Group), Phys. Rev. D **86**, 010001 (2012).
[39] D. Melikhov, Eur. Phys. J. direct C **4**, 2 (2002).
[40] Bachir Moussallam has provided us with numerical values of the kaon-pion scalar form factor for various values of the ratio f_K/f_π.
[41] B. Aubert *et al.* (BABAR Collaboration), Phys. Rev. D **79**, 072006 (2009).
[42] B. Moussallam, Eur. Phys. J. C **14**, 111 (2000). B. Moussallam sent us tables of his pion scalar form factor.
[43] R. Kamiński, L. Leśniak, and B. Loiseau, Phys. Lett. B **413**, 130 (1997).
[44] G. Barton, *Introduction to Dispersion Techniques in Field Theory* (Benjamin, New York, 1965).
[45] P. del Amo Sanchez *et al.* (BABAR Collaboration), Phys. Rev. D **82**, 111101(R) (2010).
[46] R. Aaij *et al.* (LHCb Collaboration), J. High Energy Phys. 10 (2012) 152.
[47] A. Furman, R. Kamiński, L. Leśniak, and P. Żenczykowski, Phys. Lett. B **699**, 102 (2011).
[48] G. Bonvicini *et al.* (CLEO Collaboration), Phys. Rev. D **78**, 052001 (2008).